



Published in final edited form as:

*Chem Rev.* 2008 July ; 108(7): 2554–2584. doi:10.1021/cr068081q.

## Monitoring Rapid Chemical Communication in the Brain

Donita L. Robinson, Andre Hermans, Andrew T. Seipel, and R. Mark Wightman

Department of Chemistry, University of North Carolina at Chapel Hill, Chapel Hill, NC 27599-3290

Neurotransmitters are chemicals that are secreted by neurons and relay messages to target cells. The goal of *in vivo* electrochemistry is to provide a *real-time* view of neurotransmitters in the extracellular space of the brain. This may be done in brain slices or the intact brain of anesthetized animals to probe the basic functions that regulate neurotransmitter levels. In other experiments, the measurements need to be made in the brain of *behaving* animals so that correlations of neurotransmitter fluctuations and specific behaviors can be made. For the neurotransmitter dopamine this can be accomplished today by chemical sensing of this neurotransmitter with fast scan cyclic voltammetry (FSCV) at carbon-fiber microelectrodes. Dopamine is an important target because it is a central player in the brain 'reward' system, although its precise function is not understood. Proposed roles for dopamine in reward have included the mediation of hedonia (pleasure)<sup>1</sup>, a messenger of incentive salience (wanting)<sup>2</sup>, or an error signal that promotes the learning associated with goal-directed behavior<sup>3,4</sup>. These multiple interpretations of dopaminergic function have arisen because, until recently, a real-time view of dopamine and its actions in an awake, behaving animal was unavailable. At the same time, new electrochemical technologies are being developed to measure other neurotransmitter actions. Electrochemical approaches are well suited for this application because they allow a neurotransmitter to be measured with high time resolution, enabling its precise role in the execution of behavioral tasks to be investigated.

In this review we will describe current methods to detect neurotransmitters and monitor their concentration dynamics within neural tissue. The requirements for these methods are quite stringent. They need to be sufficiently selective so that the measured responses are unequivocally due to a specific molecule. They need to be sufficiently sensitive that they can detect these substances in the physiological range. The best established methodologies are for dopamine, so the majority of the applications of the methods described herein will involve this neurotransmitter. As will be seen, the goals in measuring neurotransmitter functions are diverse. On one hand, investigators are unraveling the mechanisms that control neurotransmitter concentrations. These studies range from examining biochemical synthesis to metabolism. On the other hand, investigators are questioning how the neurotransmitter interacts with its receptors and what message it conveys. Yet a third major interest is the role of a neurotransmitter in specific behaviors. To obtain a complete view of neurotransmission and information processing, chemical sensors need to be combined with traditional neurochemical tools. We will illustrate this approach with some specific examples.

### 1. Neurotransmitters and brain function

In a recent book, the 2000 Nobel Prize winner Eric Kandel reviewed the scientific findings that lead to our current understanding of the brain<sup>5</sup>. As this book clearly shows, understanding the brain is a challenging research field, but significant progress is being made through the combined input of investigators from multiple disciplines. Kandel notes that three central principles, which emerged in the early twentieth century, form the building

blocks for modern thinking about nerve cells and brain function. Early insights came from the Spanish neuroanatomist, Cajal, who stained brain tissue and traced entire neurons at the end of the 19<sup>th</sup> century, demonstrating their projections and processes. This work established the “neuron doctrine” that has been significantly extended through modern anatomical research involving such tools as highly specific antibodies and the electron microscope. Like all cells, neurons have a cell body where the nucleus is located. They also have specialized processes for input, the dendrites, and an output process, the axon. The terminals of the axons form connections called synapses with the cell bodies and dendrites of other neurons. These synaptic regions appear poised for communication between one neuron and another.

The next major discovery was the electrical properties of neurons. Due to multiple types of ion channels, neurons can generate a rapid potential change at the cell body that can propagate down the axon. This signal, termed the action potential, occurs as a result of the encoded information from inputs to the neuron. Early pioneers in this area were Hodgkin and Huxley. They used the squid giant axon that is sufficiently large to make intracellular recordings of voltage and current with relative ease. Today this field has blossomed with the advent of patch-clamp recordings that allow the activity of individual ion channels to be observed. Furthermore, extracellular recordings of electric fields near the cell body of individual neurons, called single-unit electrophysiology, allows action potentials to be monitored while alert animals are executing complex behaviors<sup>6</sup>. The use of arrays of electrodes allows entire neuronal circuits to be monitored<sup>7</sup>.

The third principle that guides current thinking about the brain is chemical synaptic transmission. According to this principle, neurons communicate with each other at synapses by secretion of chemical substances termed neurotransmitters that interact with specific receptors, thus relaying information to downstream neurons. Evidence for this was obtained in the early twentieth century when Loewi isolated fluid from a beating frog heart and exposed it to another, nonbeating heart. The fluid induced beating in the second heart, so Loewi correctly surmised that a chemical substance in the fluid must be responsible. This later was discovered to be acetylcholine. Eccles, another pioneer in synaptic communication, initially believed that it was electrical in nature, but later was convinced of the chemical theory. He teamed up with Jaeger, the leading expert in molecular diffusion, to understand how released acetylcholine is transported to its target<sup>8</sup>. Since these initial discoveries, a number of molecules have been identified as neurotransmitters. The majority are stored in vesicles situated at nerve terminals. Action potentials cause Ca<sup>2+</sup> channels to open and the resulting Ca<sup>2+</sup> influx triggers the fusion of these vesicles with the neuronal membrane, a process termed exocytosis. Exocytosis results in release of a packet of neurotransmitters into the synapse that can then diffuse and bind to specific receptors. The receptors may be coupled to ion channels or to a second messenger system that catalyzes a cascade of chemical steps in the target cell triggered by the neurotransmitter binding.

At a fundamental level, electrochemistry has contributed significantly to one of the central aspects of the chemical communication theory, exocytosis. Exocytosis was proposed as a primary secretory mechanism in the 1960's<sup>9</sup>. However, direct chemical evidence for this process did not become available until the 1990's. The initial electrochemical experiments were done with chromaffin cells, which are cells from the adrenal gland that serve a neuroendocrine function. These cells had been shown by electron microscopy to contain vesicles and subcellular fractionation techniques had demonstrated that the catecholamine chemical messengers, epinephrine and norepinephrine, were concentrated within these vesicles<sup>10</sup>. We reasoned that exocytosis should cause a sharp concentration spike of catecholamines to appear on a small region of the cell surface, whereas any other secretory process would cause a continuous appearance at the surface of the electrode. To measure secretion, a carbon fiber electrode was placed adjacent to the cell with an applied potential

sufficient to oxidize catecholamines. When the cell was stimulated to begin secretion, sharp current spikes arising from oxidation of the secreted substances were observed, the expected result for exocytosis<sup>11</sup>. This experiment has been extended to neurons<sup>12-14</sup>, confirming the exocytotic hypothesis as a primary means of neurosecretion. Today, these types of experiments are providing dynamic information concerning the primary biochemical steps in exocytosis<sup>15</sup>.

While the understanding of chemical neurotransmission has advanced dramatically since the discoveries of Loewi due to a wide number of experimental approaches, this central principle of the brain is not as well developed as the neuron doctrine and the understanding of the electrical processes of the brain. A major impediment to understanding neurotransmitter actions was the lack of ways to observe it in real time. As will be described, observing dopamine changes in real time is now possible in an awake, behaving animal, allowing correlations to be made between animal behavioral states and a specific neurotransmitter action. The rapid development of sensors for other neurotransmitters will likely enable a much fuller picture of animal behavior and its control by chemical substances in the brain.

## 2. Non-electrochemical techniques to measure neurotransmitters within the brain

Directly assessing chemical communication between neurons in the brain of behaving animals is a long-standing goal. The most widely used approach is microdialysis, but spectroscopic techniques and *in vivo* voltammetry also provide useful information.

### 2.1. Microdialysis

A recent review by Kennedy and colleagues<sup>16</sup> reports that there are more than 9000 publications using microdialysis. In microdialysis, a perfusion fluid is pumped within a dialysis membrane implanted in the brain region of interest. Small molecules can exchange across the membrane and the interior fluid (termed the dialysate) is removed for external analysis. The microdialysis method has several advantages for measurement of brain extracellular neurotransmitters. First, it can be implemented quite easily to study a variety of neurotransmitters. Second, the chemical resolution is very good because the dialysate, which is removed from the brain, can be analyzed with a variety of techniques. Catecholamines and other easily oxidized molecules have often been quantitated by liquid chromatography with electrochemical detection, whereas amino acid neurotransmitters normally are derivatized with a fluorophore or electrophore before separation and detection.

However, there are significant problems with the technique. Microdialysis was originally thought to measure absolute concentrations of species in the extracellular fluid when used with the “no net flux” procedure<sup>17</sup> or with very slow perfusion rates<sup>18</sup>. These approaches have been questioned because the “no net flux” equilibrium position also includes a balance between the rate of the uptake and diffusion of neurochemicals through damaged tissue near the probe<sup>19</sup>. When mathematical modeling includes a term to account for transport through the damaged region, estimates of the extracellular neurotransmitter concentrations are elevated considerably<sup>20,21</sup>. Tissue damage upon insertion of a microdialysis probe is likely because its size (typically > 200  $\mu\text{m}$  in diameter) is large compared to that of nerve terminals ( $\sim 1 \mu\text{m}$ ). Histological studies have shown that brain tissue can be perturbed for over 1 mm from the implantation site<sup>22</sup>. Despite this drawback, neurotransmitter concentrations change in predictable ways with a variety of manipulations, demonstrating that information obtained with this technique does provide insights into neuronal processes<sup>16</sup>.

Most microdialysis experiments are done with a flow rate of 1  $\mu\text{L}/\text{min}$  and this typically restricts sampling to 10 min intervals so that sufficient dialysate is collected for handling and analysis. This flow rate is ideal to examine the effects of pharmacological agents on neurotransmitter levels since their transit into the brain may be slow and their effects long lasting. However, to evaluate the role of neurotransmitters on behavioral events, more rapid sampling is required. This is because neuronal action potentials underlying behavioral actions occur on a millisecond time-scale, and the neurochemistry accompanying this activity is likely to change on the same time scale. Using traditional approaches, very rapid (down to 1 min) collection of samples has been accomplished in a few experiments<sup>23–25</sup>. An alternate approach has been to couple the analytical methodology directly to the outlet of the microdialysis cannula. Using this approach, Kennedy and colleagues have achieved 14-s temporal resolution during conditioned fear experiments with microdialysis<sup>26</sup>. Extracellular glutamate and  $\gamma$ -aminobutyric acid (GABA) were rapidly increased in response to a foot shock while other putative amino acid neurotransmitters did not change. Recent advances in microdialysis sampling and detection will be discussed further in Section 11.

## 2.2. Spectroscopic approaches

Spectroscopic techniques are noninvasive and can provide spatially resolved maps of neuronal activity from the intact brain. As such, they are well suited for analysis in primates including humans. Two methods predominate today, fMRI and PET, and they both provide an indirect view of neurochemical activity. Positron emission tomography (PET) requires synthesis and administration of chemical agents that emit positrons. These are usually agonists (activators) or antagonists (inhibitors) of receptors for the neurochemical of interest. Their displacement through competition with the endogenous ligand provides insights into the brain regions that are involved in various behaviors such as addiction<sup>27</sup>. Functional magnetic imaging (fMRI) takes advantage of hydrogen spins and can provide resolution in human subjects of approximately 4 mm. In fMRI, researchers use the blood oxygen-level-dependent signal to indicate neuronal activity in a particular region. The hydrogen spins are affected by the degree of oxygen occupancy of hemoglobin because this alters the local magnetic field. This technique has been used to provide strong evidence that dopamine-containing regions become activated during reward-associated behaviors in neuroeconomics<sup>28</sup>. Indeed, the images clearly indicate that the nucleus accumbens, a structure with many dopamine terminals, becomes activated during anticipation of reward (Figure 1). However, assigning the specific neurotransmitters involved in the activation requires the use of pharmacological agents.

## 3. *In vivo* voltammetry

*In vivo* electrochemistry provides another route for sampling neurotransmitters in the brain. Several neurotransmitters including dopamine, norepinephrine, epinephrine, serotonin and histamine are easily oxidized and thus can be detected with voltammetric experiments. The advantages of this approach are that the dimensions of the electrode can be quite small and the measurements can have high temporal resolution. Carbon-fiber microelectrodes, which have a diameter of 5  $\mu\text{m}$ , are the most common sensors used in this application (Figure 2). They are encased in a pulled glass capillary with 25 to 100  $\mu\text{m}$  of the fiber protruding from the glass. The small size suggests that they will cause little tissue damage and this has been confirmed to be the case after acute implantation<sup>29</sup>. The location of the tip cannot be found by histological examination at the light microscopy level, although electron microscopy reveals some damage within 1–2  $\mu\text{m}$  of the implantation site.

The original *in vivo* electrochemical experiments searching for neurotransmitters were conducted by Adams and colleagues. In their first report ascorbate was identified as a major

interference<sup>30</sup>. Indeed, the question of selectivity has been a major impediment to the widespread use of the voltammetric approach.

### 3.1. Electrochemical properties of neurotransmitters

With respect to electrochemical detection, neurotransmitters can be separated into three different categories.<sup>31</sup> The first category of neurotransmitters consists of the electrochemically active compounds such as the tyrosine derivatives dopamine, norepinephrine, and epinephrine. Many of their metabolites are also electroactive, such as 3,4-dihydroxyphenylacetic acid (DOPAC), homovanilic acid, 3-methoxytyramine, or 3,4-dihydroxyphenylalanine (*L*-DOPA). The neuroactive tryptophan derivatives are also electroactive and include 5-hydroxytryptamine (serotonin) and its precursors or metabolites like 5-hydroxyindolacetic acid, 5-hydroxyindoletryptophan or melatonin. Other electroactive neurotransmitters are histamine and adenosine. All of these compounds can be directly detected by electrochemical oxidation of the molecule. Furthermore, other electroactive substances in the brain such as ascorbic acid, uric acid, nitric oxide, molecular oxygen, or hydrogen peroxide are also readily detectable by electrochemical methods.

The second group of neurotransmitters is not inherently electroactive; thus, these compounds cannot be detected by traditional electroanalytical methods. However, those that can be oxidized by an enzymatic reaction can be measured electrochemically by coupling the enzyme reaction with electrochemical detection. Some of the neurotransmitters in this category are amino acid transmitters such as glutamate and GABA, as well as acetylcholine and its precursor choline. Glucose and lactate, compounds important in energy production in the brain, have also been detected with this indirect electrochemical approach.

Neuropeptides and some amino acid neurotransmitters form the third group of neurotransmitters. These neurotransmitters and neuromodulators cannot be detected directly in the brain with electrochemical biosensors at this time. The most prominent members of this group are some of the amino acid transmitters like glycine as well as the large group of neuroactive peptides. However, neuropeptides with electrochemically active groups such as tyrosine, tryptophan, methionine and cysteine residues can be detected electrochemically, although this is best done after their removal from the brain and separation on a chromatographic column. Microdialysis probes are typically used for the sampling of these molecules. Detection can be done with a variety of methods such as ultraviolet absorbance, fluorescence, electrochemistry or radioactive detection<sup>32</sup>. Soft ionization techniques in mass spectrometry are also employed in discovering and analyzing neuropeptides<sup>33</sup>. Particularly promising in this regard is the use of capillary liquid chromatography interfaced with tandem mass spectrometry<sup>34</sup>. Using microdialysis samples isolated from the anesthetized rat striatum, peptide samples were introduced by electrospray into the mass spectrometer. Samples were obtained before and after depolarization of the tissue with high  $K^+$ . Comparison of these samples revealed a total of 29 peptide sequences from 6 different protein precursors. Of these, 25 had not previously been identified. Several of these peptides were found to increase neuroactive amino acids when they were infused back into the brain. In another study, a novel neuropeptide has been isolated and sequenced from a ganglion in the crab with capillary liquid chromatography and electrospray ionization mass spectrometry<sup>35</sup>. The peptide was then applied to the ganglion and it was found to alter the electrophysiological properties

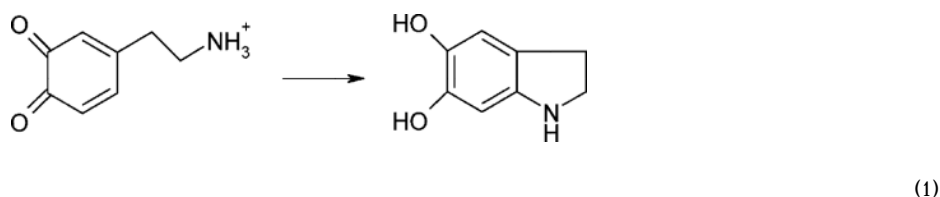
### 3.2. Electroactive neurotransmitters

Catecholamine neurotransmitters are well suited for electrochemical detection because the potential required for their oxidation is well within the potential limits for carbon and metal electrodes in physiological buffer<sup>36</sup>. True physiological buffers are chemically complex, but

they can be mimicked by an aqueous solution containing 150 mM NaCl buffered to pH 7.4 with a relatively low concentration of TRIS (~15 mM trishydroxymethylaminomethane).

Catecholamines are derived in a biosynthetic pathway from tyrosine<sup>37</sup>. The rate limiting step in the synthesis is the hydroxylation of tyrosine to L-DOPA with tyrosine hydroxylase. Dopamine is formed by the decarboxylation of L-DOPA. The major metabolites of dopamine are produced by reaction with monoamine oxidase and catechol-*O*-methyltransferase. These metabolites are DOPAC, homovanilic acid, and 3-methoxytyramine. Norepinephrine is formed after transfer of a hydroxyl group onto the  $\beta$ -position of the side chain via dopamine- $\beta$ -hydroxylase. The amine of norepinephrine can be methylated by phenylethanolamine-N-methyltransferase to form epinephrine. The action of monoamine oxidase on norepinephrine mainly produces vanilylmandelic acid and 3-methoxy-4-hydroxy-phenylethyleneglycol. As can be seen in Table 1, all of these compounds show similar 2-electron oxidation reactions with similar peak potentials at physiological pH. For this reason it is difficult to distinguish different catecholamines and their metabolites simply on the basis of their capacity for oxidation. Furthermore, many of these compounds undergo secondary reactions after the initial electron transfers. The methoxylated derivatives are oxidized at more positive potentials than the catecholamines; however, the oxidation product loses methanol and forms the *o*-quinone of the corresponding catecholamine. In the case of 3-methoxytyramine oxidation, dopamine-*o*-quinone is formed, while the oxidation of HVA leads to the formation of the oxidized form of DOPAC.

Another example for a secondary reaction is the intracyclization reaction of the oxidized hydroquinone form of catecholamines<sup>38–40</sup>.



The 5,6 dihydroxyindoline product can undergo redox-reactions itself to an aminochrome (reaction (2)). However, in the case of dopamine the rate constant for the formation reaction is very slow, on the order of  $k = 0.1 \text{ s}^{-1}$  at physiological pH. Thus, the effect of these reactions can be outrun by using fast-scan methods or measuring quickly after a potential step. The formation of the aminochrome product can be used to distinguish norepinephrine and epinephrine electrochemically since the rate of cyclization is faster for epinephrine<sup>41</sup>. In addition to this, the secondary-amine side chain of epinephrine can be oxidized at very positive potentials whereas the primary-amine side chain of norepinephrine cannot<sup>42</sup>.

The other important group of electrochemically detectable neurotransmitter and metabolites are the tryptophan derivatives including serotonin (5-hydroxytryptamine). During biosynthesis tryptophan is converted by tryptophan hydroxylase to 5-hydroxytryptophan, which then forms serotonin after decarboxylation. Metabolism of serotonin is primarily by monoamine oxidase followed by an aldehyde dehydrogenase that leads to 5-hydroxyindole acetic acid. A more minor pathway is metabolism of serotonin to form 5-hydroxytryptophenol. Tryptophan derivatives can also be oxidized and electrochemically detected in a two electron process with similar standard potentials as catecholamines. After

oxidation many different secondary reactions have been observed<sup>43</sup>. The reaction pathway is quite complicated and involves the dimerization of serotonin, as well as, after addition of water, formation of tryptamine 4–5 dione.

Histamine and adenosine are other oxidizable neurotransmitters, but to date neither has been directly detected with electrochemical methods in the brain. Histamine secretion from isolated mast cells has been detected electrochemically<sup>44</sup>. Histamine is synthesized from histidine via decarboxylation and has multiple metabolic products, such as imidazoleacetaldehyde and imidazolacetic acid. Recent research has shown that adenosine can be detected by FSCV<sup>45–48</sup>. Adenosine appears to undergo a 3-step oxidation, of which the first two steps lead to a distinct voltammogram which can be differentiated from other interferences (see Table 1).

### 3.3. Electroactive substances that interfere with neurotransmitter detection

The main electroactive interference for electrochemical measurements in the extracellular fluid of the brain is ascorbic acid. The ascorbic acid concentration in the extracellular fluid of the brain is approximately 0.5 mM, which is  $10^4$ – $10^6$  times higher than the concentrations of catecholamines<sup>49,50</sup>. Early amperometric measurements showed that the oxidation of ascorbic acid was the main signal recorded in the brain<sup>30,51</sup>. However, the electron transfer kinetics for the oxidation of ascorbic acid at carbon are very sensitive to the conditions of the electrode surface. Electrooxidation of carbon at very high potentials (~3.0 V) causes an acceleration of electron transfer rates so that the ascorbate oxidation peak occurs near its thermodynamically anticipated value. Using such treatments, Gonon and coworkers were able to show that ascorbate changed in concentration following pharmacological treatments expected to affect catecholamines<sup>52,53</sup>. This established that brain sensors for dopamine had to be able to distinguish the two molecules. This is accomplished in fast scan methods at untreated carbon electrodes because the oxidation of ascorbate shifts to more positive potentials as a result of slow electron-transfer kinetics, distinguishing the ascorbate signal from other compounds<sup>54,55</sup>. Alternatively, electrode modification with selective membranes can reject ascorbate from the electrode surface<sup>50,56,57</sup>.

Besides direct electrochemical interference, ascorbic acid can contribute indirectly to the measured signal. Ascorbate functions as the major antioxidant in the body. Thus, even when it is rendered inactive at the electrode surface, it can play a role during the electrochemical detection. For example, after the oxidation of dopamine, dopamine-*o*-quinone is reduced by ascorbate, regenerating dopamine. This catalytic reaction by ascorbic acid provides more dopamine for electrooxidation with the net result that the electrochemical current is proportional to both dopamine and ascorbate<sup>58</sup>.

### 3.4. Electrochemical detection of neuromodulators

Recently it has been shown that hydrogen peroxide plays an important role in brain signaling and neurotransmitter regulation<sup>59,60</sup>. Hydrogen peroxide can be detected directly by electrochemical methods such as amperometry<sup>61</sup>. Oxygen levels in the brain are also often determined with microelectrodes<sup>62–65</sup>. For the measurement of oxygenation of brain tissue, electrochemical methods are an alternative approach to blood oxygen-level-dependent fMRI measurements that monitor the oxygen dissociation from hemoglobin<sup>66</sup>. Although electrochemical oxygen measurements have a much better spatial and temporal resolution than fMRI techniques, many studies use fMRI techniques because of the non-invasive nature and the global spatial view that it provides. In addition, amperometric detection of hydrogen peroxide or oxygen is the basis for enzyme based electrodes that are discussed further later in Section 6.

Nitric oxide (NO), which is synthesized from arginine, has been shown to act in the central nervous system as a secondary messenger and as a mediator in the cardiovascular system<sup>37,67,68</sup>. When measuring NO electrochemically, electrodes with coatings or membranes that are specific to NO are typically used. A description of these coatings can be found later in this review (Section 4.3).

## 4. Voltammetric electrodes for neurotransmitter detection

The basis for electrochemical detection of neurotransmitters *in vivo* stemmed from the development of microelectrodes (electrodes with dimensions in micrometer range) several decades ago<sup>69</sup>. It was recognized early on that the small size, which minimizes tissue damage, also results in electrodes with a low time constant that are capable of high speed measurements. In addition, the small size minimizes distortion caused by ohmic drop.

### 4.1. Carbon electrodes

Early microelectrodes for voltammetric recordings in the central nervous system were constructed from carbon paste<sup>70–72</sup>. The carbon paste was prepared by mixing carbon powder with either Nujol or silicone oil<sup>73</sup> and then packed into the end of Teflon insulated metal microwires, resulting in disk electrodes with diameters between 100 and 300  $\mu\text{m}$ . Glass capillaries can also be filled with carbon paste. Epoxy resin is often added to the carbon paste, producing a more rigid electrode after curing<sup>74,75</sup>. Carbon paste electrodes have been reported to be stable over several months for *in vivo* applications. However, the relatively large size of carbon-paste electrodes limits the applications to larger brain regions. In addition, the larger size results in more tissue damage upon implantation in the brain in comparison to smaller sized electrodes.

Smaller carbon electrodes can be made from carbon fibers<sup>76,77</sup>. Carbon fibers can be as large as 30  $\mu\text{m}$  in diameter, but the majority of fibers range between 5–15  $\mu\text{m}$ <sup>78</sup>. Carbon fibers are prepared from the pyrolysis of either petroleum pitch or polyacrylonitrile and undergo thermal processing similar to glassy carbon. To make an electrode, the carbon fiber is inserted into a glass capillary, pulled with a pipette puller, and cut to obtain a cylindrical electrode or polished for disk electrodes. To form a well insulated seal between the carbon fiber and the glass sheath, epoxy resin is allowed to creep between the fiber and the glass and then cured<sup>79</sup>. Carbon-fiber microelectrodes constructed in this way cause minimal damage to the surrounding tissue<sup>29</sup> when inserted into the brain because the dimensions of the whole electrode including the surrounding insulation are in the lower micrometer range. Similar approaches can be used to insulate microscopic gold and platinum wires for microelectrodes.

### 4.2. Electrochemical properties of microelectrodes

The electrochemical properties of carbon electrodes depend on the oxidation state of carbon-containing functional groups of the surface. It has been proposed that surface carbonyl- and hydroxyl-groups can catalyze electron transfer for inner-sphere reactions at the electrode surface<sup>80</sup>. Furthermore, overoxidation of carbon electrode surfaces has been shown to increase the sensitivity to positively charged analytes<sup>81</sup>, due in part to increased adsorption of cations to the carbon surface<sup>82</sup>. An increase in sensitivity of 5- to 7-fold has been observed *in vitro* for dopamine when using FSCV at overoxidized carbon fibers. However, overoxidized electrodes show a slower time response and lower selectivity than electrodes which have not been exposed to high oxidative potentials. In early studies overoxidation was accomplished by repetitive excursions to + 3.0 V versus Ag/AgCl at 70 Hz<sup>52,53</sup>. Electrodes treated this way showed higher sensitivity for catecholamines, and much faster electron-transfer kinetics for ascorbate. However, in addition to increasing the amount of surface



oxides, this surface treatment seems to drastically increase the surface area of the electrode<sup>83</sup>. In modern applications, the electrode is rarely taken to potentials more positive than +1.4 V versus Ag/AgCl.

Carbon microelectrodes are well suited for direct electrochemical detection of neurotransmitters in the electroactive category for several reasons. In addition to the relatively easy and cost-effective construction, carbon electrodes show very little bio-fouling during *in vivo* applications, in contrast to metal electrodes that have to be further coated to reduce bio-fouling. Fouling of the electrode surface has a deleterious impact on electron-transfer kinetics, which can and that can distort peaks in cyclic voltammetry. Furthermore, a larger potential range can be applied to carbon electrodes than to metal electrodes which readily undergo electro-oxidation.

Gold and platinum microelectrodes have been used to directly detect catecholamines *in vitro*<sup>84-87</sup>. However, because of the relatively small potential window compared to carbon electrodes and problems with bio-fouling, metal electrodes are not commonly used for direct electrochemical detection of electroactive neurotransmitters. Platinum and gold electrodes are commonly used for enzyme electrodes to detect neurotransmitters with enzymatic catalysts *in vivo*. Micropatterning of gold and platinum onto substrates allows metal microelectrodes to be fabricated as arrays with multiple electrode sites<sup>88-90</sup>. However, in all of these applications, the noble metals are typically protected with a polymer film to prevent bio-fouling. At gold electrodes, thiol adsorption is a common problem. In brain tissue, glutathione is present at relatively high concentrations and will rapidly passivate an electrode.

When using a 3-electrode potentiostat for electrochemical measurements in the brain, the auxiliary electrode is most commonly a stainless steel electrode which is brought in contact with the surface of the brain at a convenient location. When using microelectrodes a 2-electrode setup is often used, consisting only of a working electrode and a reference electrode. Two electrode systems are preferred because the currents are sufficiently small that the polarization of the reference electrode is negligible. Also, with an extracellular NaCl concentration of ~ 150 mM, the electrolyte concentration is high enough to minimize the solution resistance. Reference electrodes are normally a small-diameter silver wire, which has been anodized in hydrochloric acid to form a silver chloride layer on the surface of the wire and implanted directly into the brain tissue<sup>91</sup>.

### 4.3. Surface modified electrodes

Different coatings have been applied to electrode surfaces to overcome some of the limitations of the electrochemical detection schemes. Surface coatings are widely employed to increase sensitivity and selectivity for certain analytes as well as to prevent surface fouling. Nafion, a perfluorinated cation-exchange polymer, is a commonly used electrode coating<sup>57</sup> for catecholamine detection because the biogenic amines are positively charged at physiological pH. Nafion can be applied by dip coating the electrode in a suspension of 2.5% Nafion in isopropanol and allowing the solvent to evaporate, leaving a Nafion film. The strong hydrophobicity of the Nafion layer minimizes surface fouling while sulfonate groups within the Nafion network promote accumulation of cations and reject anions. An alternate approach is the deposition of an overoxidized polypyrrole-film on the electrode surface<sup>92-95</sup>. These films exhibit similar properties to those described for Nafion films. However, both coatings are noncovalently attached layers that have finite thickness. The thickness means that there is a finite time required for molecules to diffuse through the coating, which increases the response time of the electrode. To remove this component, deconvolution methods have to be used to extract the real time response curves at these modified electrodes<sup>96</sup>. Carbon paste electrodes can be modified by mixing stearic acid into

the carbon paste<sup>97–99</sup>. These electrodes have been reported to have a high sensitivity and selectivity for dopamine over other electrochemical interferences present in the brain like ascorbic acid and DOPAC, although the mechanism is not understood. More recently, carbon-fiber microelectrodes have been modified by covalent attachment of molecules via diazonium salt reduction. Most commonly, the electrodes are modified with anionic functional groups like carboxyphenyl<sup>100</sup>, phenylacetate<sup>101</sup>, or sulfobenzene<sup>102</sup>. Electrodes modified in this way show a higher sensitivity and selectivity to cationic analytes such as catecholamines over anionic analytes like ascorbic acid without slowing down the time response of the detection.

Nitric oxide can be detected via direct oxidation according to the reaction scheme in Table 1. Different surface coatings have been used to create an electrode that is selectively sensitive to nitric oxide. These coatings minimize interferences from hydrogen peroxide,  $O_2^-$ , and derivatives of nitric oxide such as  $ONOO^-$  and  $NO_2^-$ , which is the main interference for these measurements. Elimination of these interferences is the biggest challenge in creating a nitric oxide sensor. Early nitric oxide sensing electrodes used a Clark-type electrode with chloroprene rubber as the NO selective membrane<sup>103</sup>. Carbon fiber microelectrodes coated with o-phenylenediamine and Nafion<sup>104</sup> also showed a very high selectivity for nitric oxide. Recent research showed that it is possible to detect the interferences  $H_2O_2$ ,  $ONOO^-$ , NO, and  $NO_2^-$  that can be distinguished by their different oxidation potentials in a potential step experiment<sup>105</sup>. Platinum-iridium electrodes coated with a nitrocellulose/pyroxylin layer were used to measure NO concentrations in various biological applications<sup>106</sup>. Recently, NO concentrations have been electrochemically detected in tumor-bearing mice with a Nafion/o-phenyldiamine coating on a platinum-iridium microelectrode<sup>107</sup>. Other approaches include electrodes modified with layers of Nafion and nickel tetrasulfonate phthalocyanine tetrasodium salt<sup>108</sup> or electrodes coated with silicone based xerogels which are doped with methoxysilanes<sup>109</sup>. However, these approaches have not yet been tested *in vivo*.

## 5. Electrochemical techniques for neurotransmitter detection

Different electrochemical techniques are used to directly detect the electroactive neurotransmitters. The most common techniques are constant-potential amperometry, chronoamperometry, differential pulse voltammetry and FSCV.

### 5.1. Amperometry

In constant-potential amperometry the working electrode is held at a DC potential sufficient to oxidize or reduce the compound of interest at the electrode surface. The presence of an electroactive species that undergoes electron transfer at this potential generates a measurable current. The integral of the current with respect to time (charge,  $Q$ ) is directly proportional to the amount ( $m$ ) of the species electrolyzed at the electrode surface by Faraday's law ( $Q = nFm$ , where  $n$  is the number of electrons in the redox step, and  $F$  is Faraday's constant). With constant-potential amperometry very high time resolution can be achieved. With a sampling rate in the kHz range, constant-potential amperometry can resolve signals on the sub-millisecond time scale. Adsorption of reactants at electrodes is not a concern with constant-potential amperometry because species are electrolyzed immediately upon contact with the electrode. For this reason adsorption processes do not slow down the response to concentration changes of the analyte as occurs with voltammetric techniques, although sensitivity tends to be lower. Collectively, these properties make constant-potential amperometry a useful technique to measure vesicular neurotransmitter release from single cells<sup>11,110–112</sup>. Studies using amperometry have allowed for attomole to zeptomole quantities of neurotransmitter secreted from single cells to be detected<sup>14,113–115</sup>.

Although amperometry can be used to determine amounts secreted, it is not particularly useful for determining concentrations. This is because the dimensions and shape of the diffusion layer must be designed to be identical during calibration and in the preparation of interest. Despite this, amperometry has been successfully used to study catecholamine concentrations in the brain and in brain slices<sup>116,117</sup>. It has been shown that the addition of ascorbic acid provides a way to obtain accurate *in vitro* calibrations for catecholamine detection<sup>118</sup>. Recall that the catalytic reaction of ascorbate with dopamine-o-quinone regenerates dopamine. If the reaction occurs at a similar rate in the calibration solution and in the brain preparation, the diffusion layer dimensions will be the same in both environments, and the calibration factor obtained *in vitro* will approximate its value *in vivo*. However, constant potential amperometry is inherently non-selective. All electroactive compounds that oxidize or reduce at the holding potential will produce a faradaic current detected at the electrode. Therefore it is important to use independent measures to identify the molecules responsible for the detected currents to confirm amperometric traces.

## 5.2. Chronoamperometry

In chronoamperometry the applied potential is instantaneously stepped from an initial potential at which no electrochemical reaction is occurring to a potential sufficient to oxidize or reduce the molecule of interest. The potential is then stepped back to the initial holding potential in a rectangular fashion. The current observed during the initial potential step is proportional to the concentration of the electroactive species present and decays with the inverse of the square root of time if the current is governed by diffusion. Traditionally the current is measured at a fixed time into the potential step and this is used to calculate the concentration of the analyte. On the step back to the initial potential, the species that were originally oxidized are reduced. From the ratio of the currents measured on the reverse and forward potential step, information about the stability of the oxidized species can be made. This feature provides chronoamperometry with somewhat greater selectivity than constant-potential amperometry. Chronoamperometry has often been used to measure neurotransmitter concentrations, especially serotonin<sup>119,120</sup> and dopamine<sup>121–123</sup>, in the extracellular fluid of the brain in real time. However, because of its limited chemical selectivity, it is most often used to measure neurotransmitter dynamics following injection of the authentic substance or an agent that immediately causes release.

## 5.3. Differential pulse voltammetry

An electrochemical method used in many early reports of *in vivo* neurotransmitter measurements is differential-pulse voltammetry. Differential-pulse voltammetry is a combination of linear sweep voltammetry with square wave techniques. The applied signal is a small amplitude square wave (~25mV) at a constant frequency superimposed on a slow linear potential ramp. The current is measured both shortly before each square wave is applied and again shortly before each pulse ends. The difference between these currents is plotted versus the potential of the linear sweep. The differential currents give a symmetric voltammetric peak whose amplitude is proportional to the concentration of the analyte. In contrast to amperometric methods, it is possible with differential-pulse voltammetry to simultaneously measure different analytes as long as the oxidation potentials of these compounds are separated by more than 100 mV<sup>32</sup>. Differential-pulse voltammetry has been used in the past for *in vivo* neurotransmitter detection of catecholamines<sup>52,124</sup> and serotonin<sup>125</sup>, as well as oxygen<sup>63</sup>. However, differential-pulse voltammetry shows a relatively poor time resolution as one scan takes longer than 30 s, whereas we now know that neurotransmitter fluctuations occur on a subsecond time scale.

#### 5.4. Fast scan cyclic voltammetry

Fast scan cyclic voltammetry (FSCV) is an electrochemical technique that provides a much higher temporal resolution than differential-pulse voltammetry but still shows high selectivity<sup>126</sup>. In FSCV the potential applied to the electrode is cycled at scan rates faster than 100 V/s in a triangular fashion (Figure 2). The voltage limits are chosen so that the reduction and oxidation of the analyte of interest lies within this potential window. At high scan rates the majority of the current detected at the working electrode is a non-faradaic current due to charging of the double layer and, depending on the material of the electrode used, redox processes at the electrode surface<sup>80,127</sup>. Typically this large background current is subtracted<sup>128</sup> so that the smaller changes in faradaic currents due to redox processes of electroactive species can be monitored. Because the background current is only stable for a brief time, FSCV is typically only used to observe concentration changes over the time course of a minute. Furthermore, because of the differential nature of the technique it is not possible to measure basal concentrations of electroactive species. FSCV has been shown to be very useful for the detection of catecholamine fluctuations *in vivo* because of the high sensitivity and selectivity<sup>129</sup>. Typically with FSCV a time resolution of 100 ms is achieved by applying the waveform for 10 ms and repeating it at 100 ms intervals. Since FSCV is a potential sweep technique, analytes with different oxidation potentials can be distinguished by their peak positions for the oxidation and the reduction as well as by their peak shape<sup>130</sup>.

In the intervals between each scan, where the electrode is typically held at a negative potential, catecholamines have been shown to adsorb to the electrode surface<sup>131</sup>. This adsorption causes a preconcentration of the catecholamine at the surface before each voltammetric scan. Anionic compounds do not show this preconcentration process; thus, this procedure enhances selectivity for cations. A further increase in selectivity is achieved by the application of high scan rates itself. Compounds with slower electron transfer rates like ascorbate can be distinguished very easily from biogenic amines at high scan rates because the oxidation of ascorbate is drawn out to higher potentials<sup>54,55</sup>.

In our laboratory, a set of background-subtracted cyclic voltammograms is collected and examined using a color representation of the current with acquisition time as the abscissa and applied voltage as the ordinate<sup>132</sup>. In this way many cyclic voltammograms can be viewed simultaneously to look for the presence of specific substances and to discriminate against electrical noise. We have taken two approaches to statistically verify identification. One procedure is to obtain cyclic voltammograms of authentic candidates suspected to be a component and evaluate their correlation of shape with the species detected *in vivo*<sup>133</sup>. A more recent approach we have adopted is to build a calibration set of suspected candidates and then evaluate the contributions of different species with principal component regression<sup>130</sup>. In this procedure, the calibration set of cyclic voltammograms obtained at different concentrations is evaluated to find the eigenvectors (principal components) that describe the data<sup>134</sup>. Only a few are needed, and thus the dimensionality of the 1000 point cyclic voltammograms can be reduced considerably. The principal eigenvector captures the maximum variation in the calibration set. The second eigenvector captures additional variance not described by the first eigenvector. This process is continued until all the relevant information is captured. Next a regression matrix is calculated that provides the necessary scaling factors for the retained principal components. The cyclic voltammograms obtained during the experimental situation are then resolved into components at their respective concentrations using the eigenvectors and the regression matrix. This procedure results in separate traces for each chemical species used in the calibration set and an error signal, the residual. We accept the results of the analysis as long as the residual remains smaller than the level set by the 95% confidence limit<sup>135</sup>. If a species is present in the experimental results but not in the calibration set, it will be included in the residual along with noise and other interferences.

### 5.5. pH electrodes for *in vivo* use

Fluctuations in pH in discrete brain regions have been shown to follow electrical stimulation of dopamine neurons and seem to be an indirect measure of metabolism coupled to blood vessel dilation and oxygenation of the tissue<sup>64</sup>. Microelectrodes to measure pH in the brain have been developed with different approaches. One approach utilizes double barreled, thin wall capillary glass<sup>136–138</sup>. The pH sensitive barrel is filled with a hydrogen ionophore cocktail to provide a liquid pH sensitive junction. The hydrophobic cocktail functions in a way that is analogous to the glass membrane of a traditional glass electrode. The second barrel is traditionally the reference barrel and is filled with a buffer solution at physiological pH. The electrodes are used in a potentiometric mode with the voltage difference between the two electrodes measured. Electrodes produced in this fashion have been shown to resolve at least 0.001 pH units in a millisecond time scale<sup>136</sup>.

A different approach uses metal microelectrodes as micro-pH sensors. Most commonly iridium-oxide has been used as the electrode material. Iridium oxide electrodes show a linear sensitivity over a pH range of 2 – 10, exhibit low susceptibility to other cationic interferences, and seem to function under *in vivo* conditions<sup>139,140</sup>. Anhydrous iridium oxides have Nernstian responses to pH changes that originate from the reactions between the +III and the +IV states of iridium:



Because the redox potential for both reactions (3) and (4) is dependent on the pH of the solution, the pH-measurement can be made potentiometrically *versus* a Ag/AgCl reference electrode. Recent research has shown that iridium-oxide pH sensors can be patterned in a microelectrode array to allow simultaneous recording at multiple sites<sup>141</sup>.

*In vivo* pH changes can also be measured with background subtracted FSCV at carbon electrodes<sup>64,142,143</sup>. Carbon-fiber electrodes respond to pH changes because one of the contributions to the background current is electrolysis of oxide groups on the electrode surface. The electrolysis is pH dependent, and a differential signal is observed when the pH changes as a consequence of the background subtraction procedure. The amplitude of this change is directly proportional to the amplitude of the pH change.

## 6. Enzyme electrodes for detection of neurotransmitters

Considerable research has been conducted over the last couple of decades to design electrochemical sensors for molecules that are not electroactive. These sensors rely on the principle that during the oxidation of an analyte by an enzymatic reaction an electroactive species is formed that can be detected at the electrode surface (Figure 3). With this technique electrochemical sensors that measure glucose and lactate concentrations in the brain have been constructed to study brain metabolism. The design features of these electrodes have been adapted to detect glutamate, choline, acetylcholine, GABA and adenosine<sup>144,145</sup>. Detection with enzyme electrodes normally utilizes amperometric detection. Thus, it is important to construct electrodes with selective membranes to minimize interfering signals<sup>146</sup>.

## 6.1. Design principles of electrodes for metabolic substrates

An important driving force for the development of enzyme electrodes was the need for a reliable glucose sensor for blood measurements in diabetic patients. The first enzyme-based glucose-sensing electrodes were developed in the 1960's<sup>147,148</sup> by immobilizing glucose oxidase embedded in a gel-matrix on a Clark-type oxygen electrode. The enzymatic reaction turns glucose into gluconic acid with consumption of oxygen.



The configuration of the sensor depends on whether reaction (5) is monitored by measuring hydrogen peroxide production or oxygen consumption, both of which can be detected by their electrochemical reduction. When oxygen is measured a low reducing potential is required for amperometric detection. This eliminates interferences because only a few endogenous electroactive species undergo electron transfer in this potential region. However, hydrogen peroxide detection by its oxidation is often used, although the relatively high potential (0.6 V versus Ag/AgCl) that is applied to the electrode significantly increases the number of interfering electron donors. Redox mediators are commonly horseradish peroxidase coupled to an osmium complex, ferrocene, or polypyrrole<sup>149–150</sup> to enable the use of lower applied potentials (0 V versus Ag/AgCl). This way the interferences by endogenous species can be minimized. However, the presence of oxygen can cause interferences itself at a redox-mediated electrode. If the reaction of the redox-mediator with the reduced enzyme is relatively slow compared to the reaction of the enzyme with oxygen directly, low sensitivity will result. Therefore, mediators that react rapidly with the reduced enzyme are desired or selective gas membranes have to be used for the construction of the electrode.<sup>151</sup>

Miniaturized glucose sensors based on hydrogen peroxide sensing have been developed for subcutaneous monitoring<sup>152</sup>, as well as for direct measurements in the brain<sup>153,154</sup> to study brain metabolism<sup>155</sup>. Lactate oxidase<sup>156–158</sup> can also be used as the reactive enzyme to obtain further information about brain metabolism:



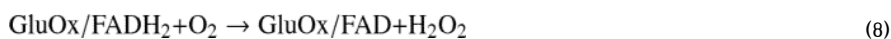
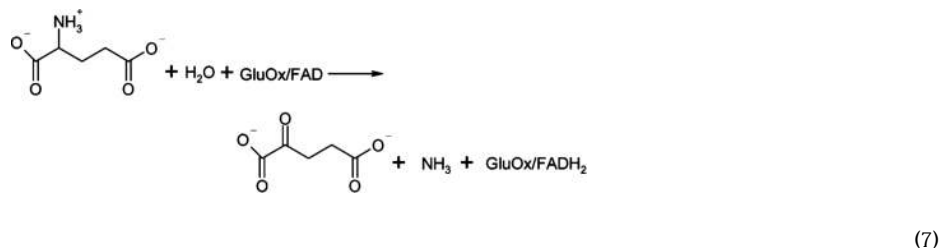
A critical component for both glucose and lactate sensors is the availability of molecular oxygen. Because of active respiration within the brain, free oxygen concentrations are lower than 50  $\mu\text{M}$ .<sup>159</sup> Therefore, membranes over the surface of the sensor serve to restrict the flux of analyte so that the oxygen is not completely depleted during detection. Electrochemical glucose and lactate detectors have also been used with microdialysis probes that allow removal of extracellular fluid for on-line, high-resolution detection outside of the brain<sup>160,161</sup>.

## 6.2. Adaptation of sensor technology for neurotransmitters

The developments in the field of glucose sensors have been exploited to develop electrochemical detectors for neurotransmitters. Glutamic acid, or glutamate, is the major excitatory neurotransmitter in the central nervous system. It is synthesized from glutamine in glial cells where it is converted by glutaminase into glutamate. Alternatively it is synthesized from glucose via the Krebs cycle. Most electrochemical glutamate sensors have been constructed from metal electrodes, most commonly platinum coated with a thin layer of electropolymerized o-phenylenediamine<sup>162</sup> or Nafion. These surface-coated polymers minimize interferences, especially anionic compounds. Glutamate oxidase, the enzyme that

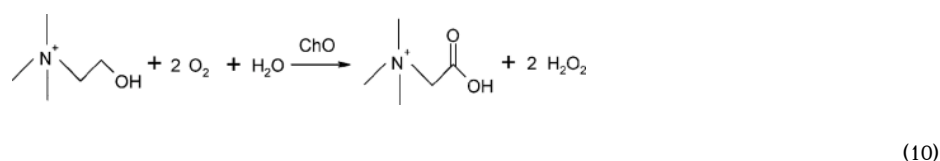
breaks down glutamate in a layer of BSA and glutaraldehyde on top of the Nafion layer<sup>89,90,163–166</sup>.

All these electrodes follow the basic electrochemical detection scheme for glutamate (7 to 9) as described by Kusakabe<sup>167</sup>:



The first two steps of this reaction scheme occur in the outer enzyme-containing layer. The hydrogen peroxide that is generated in reaction (8) then diffuses through the selective membrane to the electrode surface where it gets oxidized in a two-electron process (reaction 9). Glutamate electrodes currently exhibit a detection limit of around 1  $\mu\text{M}$  and a linear range up to 200  $\mu\text{M}$  for *in vitro* calibrations<sup>90</sup>.

The neurotransmitter acetylcholine is synthesized *in vivo* from choline by choline acetyltransferase. Electrodes designed for the detection of choline are similar to those described for glutamate detection<sup>168,169</sup>. Instead of glutamate oxidase, choline oxidase is immobilized. The first reaction step is shown in the following reaction scheme:



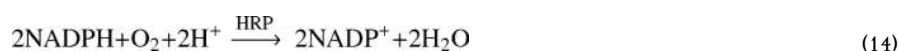
Hydrogen peroxide can either be detected directly at the electrode<sup>170</sup> as shown in reaction (9). To monitor acetylcholine concentrations, acetylcholine esterase is added to the electrode surface to convert acetylcholine to choline:



Choline is then oxidized according to reaction (10), which then leads to reaction (9). Because choline is present in the brain as well as being one of the products in the reaction cascade, it is important to have an independent measure of choline. This can be done in a differential manner by subtracting the signal from a choline sensor from the overall signal recorded at the acetylcholine sensitive electrode<sup>170,171</sup>. For this measurement, it is important to carefully match the response of the two sensors to choline because the concentration of choline in the brain can be two orders of magnitude higher than

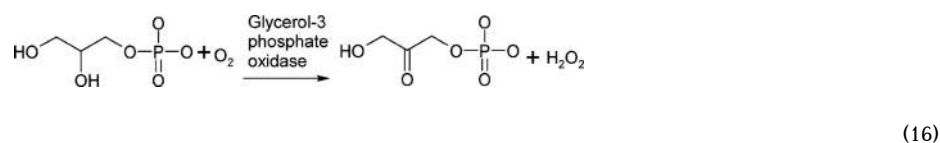
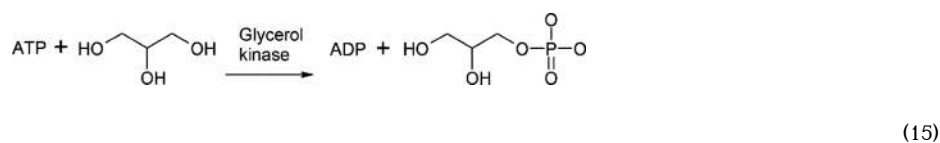
acetylcholine concentrations. However, in at least one documented example, a choline sensor adsorbed enough acetylcholine esterase that it became sensitive to acetylcholine<sup>172</sup>.

Another neurotransmitter that can be detected electrochemically after an enzymatic reaction is the inhibitory amino acid transmitter  $\gamma$ -aminobutyric acid (GABA). Glutamate is the biochemical precursor for GABA. GABA is formed after  $\alpha$ -decarboxylation of glutamate. The bioenzymatic system used for GABA detection is comprised of the enzymes GABA- $\alpha$ -oxoglutarate transaminase (GABA-T) and succinic semialdehyde dehydrogenase (SSDH)<sup>173,174</sup>:



The reaction for the electrochemical detection of GABA is a three-step process. The product of the first two enzymatic reactions (12 + 13) is NADHP, which is formed from  $\text{NADP}^+$  embedded in the enzyme layer. NADHP is then re-oxidized to  $\text{NADP}^+$  after reacting with horseradish peroxidase. The amperometric detection is based on oxygen consumption in reaction (14). However, to date GABA electrodes have been used little for direct *in vivo* applications. GABA detection is primarily conducted by separation methods after microdialysis.

In addition to direct electrochemical detection<sup>48</sup>, purines such as ATP, ADP, and adenosine<sup>175</sup> have been detected *in vivo* with enzyme electrodes<sup>176</sup>. ATP sensors have been constructed by combining glucose oxidase and hexokinase. The signal recorded for changes in ATP is due to the reduction in the glucose signal via phosphorylation of glucose to glucose 6-phosphate<sup>177,178</sup>. A different detection scheme relies on the phosphorylation of glycerol<sup>174,179</sup>.



This detection scheme again utilizes the amperometric detection of hydrogen peroxide at the electrode.



To further eliminate interferences in the amperometric signal, self-referencing electrodes have been developed<sup>89,90</sup>. With this electrode setup two electrodes are placed within a very close proximity to each other by constructing the microelectrodes via photolithographic etching. Only one of the electrodes sites is coated with the enzymatic coating, while the other site is coated in the same manner but without addition of the enzyme. This non-enzyme-containing electrode serves as a reference electrode that can sense all electrochemical signals originating from interfering species. The signal is then subtracted from the signal measured at the enzymatic electrode to obtain a signal that is purely due to the analyte of interest. This method can be applied to all types of enzyme electrodes described here. However, the prerequisite for this technique is that the chemical environment is identical at each of the two electrode sites and that both electrodes have identical sensitivities to interferences.

## 7. Aspects of chemical communication revealed via electrochemical techniques

Once a sensor is constructed and a neurotransmitter of interest can be reliably detected, a number of questions and issues can be addressed concerning the neurotransmitter. For example, how is a particular neurotransmitter transported through the extracellular space? What factors regulate its concentration? What is its lifetime outside of a neuron? How is it affected by pharmacological agents? How does it interact with its receptors? These questions are currently being addressed for dopamine. In the future, these same issues will need to be addressed with the enzymatic sensors that allow many more neurotransmitters to be examined.

### 7.1. Dopamine diffusion and uptake

Just as in a quiescent solution, diffusion plays the dominant role in the mass transport of dopamine and other small molecules within the extracellular space of the brain. Understanding diffusion of neurotransmitters is important because it dictates how far they can traverse from their release site and interact with receptors. In seminal studies, Nicholson introduced substances into the brain using iontophoresis (see section 9.2 for a discussion of this technique), which were then detected with ion selective electrodes<sup>180</sup>. Tetramethylammonium ion was used extensively as a probe ion because it has few specific interactions with brain tissue and, thus, its rate of arrival at the sensing electrode was predominantly due to diffusion. These studies showed that diffusion in the extracellular space has two features that cause it to be different from diffusion in solution. First, dilution is not as great as it is in solution because of the reduced volume fraction of the extracellular fluid. Surprisingly, however, the fraction that is extracellular fluid in the brain is quite large, approximately 20% of the total volume. Second, the rate of diffusion in the extracellular fluid is affected by tortuosity. The presence of neurons, glia, blood vessels and other cells make a tortuous path that effectively slows the diffusional rate. Quantitative measurements show that diffusion coefficients have a value in the brain that is approximately one third of their solution values as a result of the tortuosity.

In early experiments, our laboratory injected dopamine into a brain slice that was maintained in an active metabolic state, and we attempted to monitor dopamine following its diffusion to the electrode<sup>181</sup>. Interestingly, we were unable to detect any injected dopamine in the caudate nucleus, a brain region in which dopamine is a neurotransmitter, but we were able to detect it using identical methodology in a brain region that did not contain dopaminergic nerve terminals (Figure 4). Subsequent experiments showed that the failure to see dopamine reach the electrode in the caudate nucleus was because the dopamine transporter removed it from the extracellular space before it could reach the electrode. This did not occur in brain

regions that lacked the transporter. In the caudate nucleus, addition of the competitive inhibitor of the dopamine transporter, nomifensine, allowed dopamine diffusion to be observed. These experiments established that mass transport of dopamine in the brain is actually a competition between uptake, which removes dopamine from the extracellular fluid, and diffusion, which dilutes its concentration.

Uptake by the dopamine transporter follows the Michaelis-Menten equation<sup>182</sup>. Thus, at high concentrations dopamine is transported into terminals at a rate that is linear with time and that is given by the maximum velocity,  $V_{\max}$ . Of all the brain regions tested in the rat, the  $V_{\max}$  is largest in the caudate nucleus with a value of 4  $\mu\text{M/s}$  and smallest in regions with less transporter density. In contrast, the  $K_m$  for uptake is approximately 200 nM in all regions. This value is of interest because enzymes exhibit  $K_m$  values slightly greater than the concentrations they are expected to experience under physiological conditions. The dominance of dopamine uptake was more recently demonstrated by monitoring the clearance of endogenous dopamine in transgenic mice lacking the dopamine transporter. Dopamine clearance in the transporter knock-out mice was 100 times slower than in tissue from wild-type mice<sup>183</sup>.

A complete description of the interaction of dopamine diffusion and uptake in the brain requires that one solve the relevant diffusion equations coupled to the Michaelis-Menten equation to account for uptake. Nicholson has presented a numerical solution to this problem for introduction of dopamine from a point source<sup>184</sup>. This work has shown that near the point of delivery uptake is saturated, and the competition between  $V_{\max}$  and diffusion predominates. However, at distances further from the source, the concentration of dopamine rapidly drops as the transporter becomes unsaturated due to dilution of the initial concentration by the combined effects of diffusion and uptake. Under these conditions, the concentration profile resembles behavior for diffusion competing with first order kinetics that has a rate constant given by  $V_{\max}/K_m$ . Figure 5 (top) illustrates this with a high concentration at 0–10 s (during application) and 0–100  $\mu\text{m}$ , while thereafter concentration drops as uptake removes dopamine from the extracellular space. The dopamine concentration extends in both time and space when uptake is inhibited by nomifensine (middle, a competitive uptake inhibitor) or completely absent (bottom). Cragg and Rice have used this limiting form to model release from single nerve terminals firing alone and have emphasized that dopamine concentrations reach very low values after a short distance because of these competing processes<sup>185</sup>. However, it is important to note that if adjacent nerve terminals release dopamine simultaneously the point source approximation no longer holds. These more complex conditions have been modeled with finite difference simulations that account for the coupling of uptake and diffusion<sup>186</sup>. The simulations reveal that dopamine concentration is less diluted than in the case of a point source and can diffuse farther at concentrations sufficient to interact with dopamine receptors. Nevertheless, the diffusion distance is still only a few micrometers.

## 7.2. Modeling dopamine release and uptake

Release from nerve terminals is the physiological way in which dopamine enters the extracellular fluid. Early approaches to elicit release used chemical stimulation. However, a better approach is to take advantage of the electrical properties of neurons. Action potentials can be evoked with brief trains of millisecond-wide pulses. The electrical stimulation provides a distinct, time-locked stimulus that can be applied to discrete brain regions to evoke dopamine release. Upon stimulus termination, the restoration of dopamine concentrations to their prestimulus value can be observed. As discussed above, the lifetime of dopamine in the extracellular space on the second time scale is clearly affected by uptake and diffusion. Metabolism plays a role on a longer time scale<sup>187</sup>.

We adopted this approach in the 1980's and the resulting data were interpreted with a relatively simple model. If uptake by the dopamine transporter is primarily responsible for the removal of dopamine from the extracellular kinetics, then it should follow Michaelis-Menten kinetics as established in preparations of isolated nerve terminals. Thus, when measured as a function of time, the disappearance of dopamine after the stimulation should obey the following equation:

$$[DA](t) = \int_0^t \frac{V_{\max} dt}{(K_m/[DA]) + 1} \quad (17)$$

where  $V_{\max}$  is the maximal rate of dopamine uptake and  $K_m$  is the Michaelis constant that has been determined by independent methods to have a value of  $0.2 \mu\text{M}$ <sup>188</sup>. The *in vivo* data was found to follow this predicted behavior. During the stimulation, we assumed that each stimulus pulse in a train evoked a spatially uniform concentration change in extracellular dopamine, and that this concentration was lowered by the transporter, again following Michaelis-Menten kinetics<sup>189</sup>. The expected behavior during the stimulation is therefore:

$$[DA](t) = \sum_{j=1}^n [DA]_{p,j} - \int_0^{\tau} \frac{V_{\max} dt}{(K_m/[DA]) + 1} \quad (18)$$

where  $[DA](t)$  is the dopamine concentration during a stimulation composed of  $n$  pulses and that has a duration,  $\tau$ .  $[DA]_p$  is the concentration of dopamine evoked by each stimulus pulse. Because the electrical stimulation forces a large population of dopamine neurons to fire, we assumed that dopamine concentration gradients were minimal so that diffusion could be ignored. However, the concentrations reported by the electrode were distorted by the limited response time of the electrode, which arose from diffusion through Nafion coatings<sup>190</sup> or the kinetics of dopamine adsorption/desorption at uncoated electrodes<sup>131</sup>.

This model has been used extensively to characterize endogenous dopamine release and uptake, as well as effects of pharmacological agents on these processes<sup>191</sup>. For example, cocaine slows down the uptake portion of the observed response, consistent with its role as a dopamine uptake inhibitor (Figure 6). Haloperidol, a neuroleptic drug used in the treatment of schizophrenia, alters the amount of dopamine released per stimulus pulse. The model correctly predicts that the concentration of extracellular dopamine evoked by a low (5 Hz) frequency stimulus rapidly achieves a steady-state level during the stimulation whereas a high frequency (60 Hz) stimulus causes the dopamine concentration to increase during the stimulation. The latter result occurs because the rate of release greatly exceeds the rate of uptake. In contrast, the steady-state response at low frequency stimulations is simply a consequence of a slight imbalance in these two parameters. The model also successfully describes norepinephrine release evoked by electrical stimulation<sup>192</sup> as well as the dynamics of 5-HT release<sup>193</sup>. Recently developed software allows extraction of kinetic parameters for uptake and release using a Simplex optimization routine<sup>194</sup>.

Nevertheless, in evaluating this model it quickly became clear that it could only describe dopamine release under a limited set of conditions. The assumption of constant dopamine release per stimulus pulse failed with long stimulation trains. Furthermore, to achieve reproducible amplitudes some interval of time had to occur between consecutive stimulation trains<sup>195,196</sup>. Thus, Justice and coworkers developed a more complete model that alleviated one of these limitations<sup>197</sup>. They recognized that dopamine is stored within two 'pools' of presynaptic vesicles that have been termed the readily releasable and the reserve pools. The

Justice model explains that the delay required between consecutive stimulation trains is necessary to allow the reserve pool to refill the readily releasable pool. By incorporating this reserve compartment into the model, it was able to accurately describe release and uptake over a broader range of conditions. Recent experiments suggest that the reserve pool is segregated from the releasable pool by the protein synapsin<sup>198,199</sup>. This vesicle-binding protein appears to sequester vesicles away from sites where they can undergo exocytosis.

Interest in the modeling of dopamine release and uptake has recently been renewed due to unexpected results from behavioral experiments. Rats will press a lever coupled to instrumentation that electrically stimulates their dopamine neurons using pulse trains similar to those used in the characterization experiments<sup>200</sup>. Apparently, the response is rewarding because the animals will press the lever for extended periods of time, ignoring food and water. However, the extracellular dopamine release profiles observed during these stimulations differ from the predictions of the simple 'Wightman' model described above (eqn. 18). For example, during continuous lever pressing, the evoked dopamine concentrations decrease, eventually reaching undetectable levels. To address this issues, Montague and colleagues<sup>201</sup> derived a dynamic model of dopamine release that included three independent adaptive processes. These components – a short-lasting facilitation, a short-lasting depression, and a longer-lasting depression – fit the changing amplitude of dopamine release events elicited by a variety of stimulus patterns in awake and anesthetized rats (Figure 7) without the need to adjust the values of  $K_m$  and  $V_{max}$  for uptake. Moreover, the mechanisms underlying each component were suggested to be well-described terminal processes. For example, the long-lasting depression may be linked to the rate of dopamine biosynthesis and the mobilization of vesicles in the reserve pool to the readily releasable pool of dopamine vesicles<sup>196,202</sup>, processes described by Justice in his original model.

The short-term depression component indicated in Montague's model operates on a similar time scale to negative feedback from dopamine D2 autoreceptors, receptors on dopamine nerve terminals that are responsive to dopamine<sup>203</sup>. Binding of dopamine to the autoreceptors decreases both dopamine synthesis and release probability due to activation of intracellular second messenger cascades. Kita and colleagues<sup>204</sup> directly tested whether the short-term depression component resulted from dopamine autoreceptor activation. First, the effect of an initial stimulation train on dopamine neurons on a subsequent train was tested by varying the delay between the two; the closer the second train followed the first, the smaller the amplitude of the resulting dopamine release event. Consistent with earlier studies<sup>203,205</sup>, blocking D2 autoreceptor activity with haloperidol both increased the amplitude of the dopamine signal at the first stimulation train (revealing a tonic control of dopamine release by D2 receptors) and increased the amplitude of the dopamine signal at the second train. This confirmed classic autoreceptor effects to suppress dopamine release. Next, we examined drug effects on more complex patterns of stimulation trains. Both raclopride, a D2 antagonist (inhibitor), and quinpirole, a D2 agonist (activator), modulated the initial stimulus train in predictable ways (amplification and attenuation, respectively). However, their effects on subsequent stimulations were more complex. While raclopride removed the short-term depression component indicated by Montague's model, it also removed the short-term facilitation. Conversely, the D2 agonist quinpirole amplified both components. This paradoxical finding that D2 receptor activation underlies both depression and facilitation of dynamic dopamine release may be explained by a rapid desensitization process: that is, while the initial effect of D2 activation is to decrease subsequent dopamine release, this process quickly desensitizes, and the desensitization manifests itself as an apparent facilitation<sup>204</sup>.

How much does our understanding of electrically stimulated release, in which many neurons simultaneously fire, translate to insight of *physiological* dopamine transmission? In fact, it

has been more useful than originally expected. First, electrophysiological recordings of dopamine neurons in primates reveal that approximately 75% of dopamine neurons exhibit increased firing rates at the presentation of salient stimuli<sup>206</sup>, suggesting synchronous firing under some conditions. Moreover, electrical coupling of dopamine neurons via gap junctions<sup>207</sup> may promote coincidence during firing in bursts<sup>208</sup>. Finally, the validity of models of stimulated release has been implicated by the occurrence of *dopamine transients*: brief, high concentrations of dopamine that naturally occur *in vivo*, likely result from burst firing of dopamine neurons, and can be pharmacologically manipulated in a manner consistent with stimulated release.

## 8. Phasic dopamine transmission *in vivo*

In recent years, many studies have used FSCV to measure brief, local fluctuations of dopamine occurring *in vivo* in rats that are freely moving and unrestrained. The transition from measurement of dopamine signals that were electrically evoked to naturally occurring was possible due to increased sensitivity of both electrodes and instrumentation<sup>209</sup>.

However, present studies now reveal that spontaneous transients are absent in animals anesthetized with urethane<sup>210</sup> and only occur in the awake state. Thus, experiments in freely moving animals have been especially significant in that they provide a window on dynamic dopamine chemistry that can be directly associated with learning and motivated behavior.

### 8.1. Measurements in freely moving rats

Taking the procedures and approaches that were used in anesthetized animals and adapting them for freely moving rats required several developments. First, because the carbon-fiber microelectrodes were thought likely to fail when chronically implanted, a procedure had to be devised to insert a fresh electrode each day. Rebec and colleagues devised a micromanipulator that could be fitted on the skull and could be used to lower the electrode down into the brain region of interest. Their initial experiments with this approach revealed a transient surge of dopamine when a rat was exposed to a new environment<sup>211</sup>.

In our own laboratory, we rapidly adapted this technology. In addition, surface mount operational amplifiers were used to construct a current transducer that fit directly on the animal's head<sup>212</sup>. Special precautions have to be taken to eliminate noise associated with the wires and commutator that allow the animal to freely move around the behavioral chamber. The procedures are now well documented<sup>91</sup>, and measurements in freely moving animals are more commonplace than they were just 10 years ago.

### 8.2. Basal rates of dopamine transients

The initial measurements of naturally occurring dopamine transients were made at the presentation of highly salient stimuli to the rat, such as another rat<sup>213</sup> (Figure 8). These stimuli were predicted to induce synchronized burst firing of dopamine neurons that would result in dopamine transients. However, a subsequent study revealed that dopamine transients also occurred throughout the dorsal and ventral striatum (i.e., dopamine release sites in the forebrain) *in the absence of obvious external stimuli*<sup>214</sup>. Later studies confirmed these unexpected results. Notably, as detection limits have decreased with improved instrumentation and technique, the observation of dopamine transients at baseline has become more frequent and the average amplitude of these signals has decreased. Current studies report that dopamine transients occur at  $> 1 \text{ min}^{-1}$  in the nucleus accumbens during baseline with a mean maximal concentration of 40 – 50 nM<sup>209</sup>, although the distribution of the maximal concentrations suggests that even smaller fluctuations occur<sup>215</sup>.

However, discussion of average frequency rates of dopamine transients masks the dramatic heterogeneity observed across multiple recording sites, even within the same rat. As the

carbon fiber electrode used in these experiments is small, typically a  $6 \times 100 \mu\text{m}$  cylinder, it is measuring from a finite number of dopamine release sites. Dopamine terminals are approximately  $4 \mu\text{m}$  apart in the striatum<sup>216</sup> and, thus, the microelectrode is likely monitoring release events from only a few dopamine neurons. Moreover, these neurons can vary widely in their propensity to fire in bursts<sup>217</sup>, the firing pattern that presumably produces dopamine transients. As a result, some recording sites in the nucleus accumbens produce high frequencies of dopamine transients, while others yield few or no transients even when electrically-stimulated release is robust (indicating the proximity of functional release sites)<sup>215</sup>. Nevertheless, when transients are detected, they are typically of similar amplitude and duration regardless of the basal frequency (Figure 9).

### 8.3. Drug effects on rates of dopamine transients

Dopamine transients can be pharmacologically manipulated by drugs that directly or indirectly target dopamine transmission. Drugs that block dopamine uptake, such as nomifensine and cocaine, increase both the frequency and size of dopamine transients; the amplitude and duration of transients are enhanced in a manner consistent with their effects on electrically stimulated dopamine signals<sup>218–220</sup>. The cannabinoid agonist WIN55,212-2 also increases the frequency and amplitude of dopamine transients<sup>221</sup>, but via different mechanisms: CB1 receptor activation by WIN55,212-2 on presynaptic GABA terminals in the ventral tegmental area (a brain region that contains cell bodies of dopamine neurons) reduces GABA transmission and, thus, disinhibits postsynaptic dopamine cell bodies, resulting in increased burst firing of dopamine neurons<sup>222,223</sup>. Similarly, nicotine boosts the frequency and amplitude of dopamine transients<sup>224</sup>, which may be due to both enhanced burst firing of dopamine neurons<sup>225</sup> and enhanced calcium-dependent dopamine release at the terminals<sup>226</sup>. In contrast, ethanol increases the frequency of dopamine transients only in a subset of recording sites (“ethanol-responsive sites”)<sup>224</sup>.

In addition to detecting changes in transient frequency, FSCV has revealed short-term changes in tonic dopamine levels following drug administration. Cocaine, nicotine, and ethanol can all induce gradual increases in dopamine levels (over tens of seconds) on which individual dopamine transients are superimposed<sup>218,224</sup>. With cocaine, these slower surges of dopamine are dose-dependent<sup>218</sup>.

Not every site within the nucleus accumbens is equally sensitive to these various drugs. As mentioned above, ethanol induces dopamine transients only at some recording sites within the accumbens, with other sites yielding no clear change in transient rates<sup>224</sup>. The heterogeneous effects of ethanol may reflect the sensitivity of subsets of dopamine neurons to fire in bursts in response to this drug<sup>227–229</sup>. Site-specific variation has also been reported for cocaine. Specifically, more transients are observed at release sites that already yield dopamine transients, whereas in sites devoid of transients (but containing dopamine release sites as evidenced by electrically stimulated release) no additional transients are induced by cocaine<sup>215</sup>. This finding suggests that a major mechanism by which cocaine increases transient frequency is to amplify ongoing dopamine transients as opposed to triggering the occurrence of additional transients, consistent with cocaine’s primary effects at the terminal rather than the cell body.

### 8.4. Dopamine transients during learning and reinforcement

A rich area of psychological research has focused on cognitive mechanisms of learning and reinforcement<sup>230</sup>. Certain objects or experiences are rewarding or reinforcing, and animals readily learn that environmental cues can signal future availability of rewards. In order to make the association between the environmental cue, or conditioned stimulus (CS), and the reward, or unconditioned stimulus (US), an element of surprise is necessary. In other words,

learning occurs when the US is unexpected. In contrast, if the US is always predicted by a CS (and the animal has learned this), no additional learning occurs. The predictability of the US can be described as prediction error  $(\lambda - \Sigma V)^{231,232}$ , in which  $\lambda$  is the maximum amount of learning or prediction that can be achieved of the predictability of the US, and  $\Sigma V$  is the sum of the amount of learning (or prediction) that actually occurred at a given presentation of the US. Thus, when the US is completely unexpected,  $\Sigma V = 0$  and the prediction error equals  $\lambda$ . Conversely, when the US is fully expected,  $\Sigma V = \lambda$  and the prediction error is zero.

Is it possible that a single set of neurons could encode this prediction error in its activity? Electrophysiological studies of dopamine neurons suggest that this is so<sup>206,232</sup>. For example, the majority of dopamine neurons in the monkey midbrain show a brief increase in firing rate at the unexpected presentation of a reward ( $\Sigma V = 0$ )<sup>233</sup>. Moreover, when the reward is fully predicted by a CS ( $\Sigma V = \lambda$ ), the dopamine cells no longer increase firing at the reward, but rather at the presentation of the CS, which itself was unexpected<sup>233</sup>. Omission errors, i.e., the unexpected omissions of rewards that were fully predicted by a CS, are also encoded by dopamine neurons with an inhibition of firing at the time that the reward would have occurred<sup>206,234</sup>. Finally, the excitation of dopamine neurons in response to both an unexpected reward and a CS predicting a reward vary in intensity with the magnitude of the actual or predicted reward<sup>3</sup>.

While the firing rates of dopamine neurons appear to encode prediction error for rewards, it is not a certainty that dopamine release at the terminal follows suit. Local influences on dopamine release<sup>185,235,236</sup>, as well as facilitation and depression mechanisms triggered by recent action potentials<sup>201</sup>, can induce a mismatch between neuronal firing and dopamine release<sup>237</sup>. Thus, fast electrochemical techniques are necessary to examine dopamine release in specific terminal regions during learning and reinforcement.

The hypothesis of dopamine as a learning signal for reward first predicts that dopamine release would occur at the unexpected presentation of reinforcing stimuli. Indeed, the earliest measurements of dopamine transients were at the presentation of novel and reinforcing stimuli<sup>211,213,214,219</sup>, a response that habituated as the presentations became more predictable<sup>214</sup>.

A second prediction is that dopamine release would occur at the unexpected presentation of stimuli that forecast a reward, i.e. a CS. To determine this, dopamine release in response to a CS associated with cocaine was measured. Rats were trained to self-administer cocaine by pressing a lever in an operant box. At each lever press, a multimodal stimulus (light, tone and lever retraction) was activated along with the cocaine infusion. When dopamine was monitored with FSCV, dopamine transients were observed time-locked to the lever press (Figure 10), with the maximal concentration occurring 1.5 s after the press<sup>238</sup>. Was the signal due to pressing the lever, a pharmacological effect of cocaine, or the presentation of the cues? Several pieces of evidence support that the transient was associated with cues, which were serving as a CS for cocaine. First, when the multimodal stimulus was presented noncontingently (i.e., apart from the rat pressing the lever), a dopamine transient was elicited<sup>238</sup>. Second, noncontingently-delivered cocaine in a group of untrained rats demonstrated that dopamine transients induced by the pharmacological effects of cocaine were only detected > 30 s after the lever press/infusion<sup>220</sup>. Finally, when rats underwent extinction – that is, lever pressing elicited the multimodal stimulus but saline was delivered instead of cocaine – the dopamine transients time-locked to the lever press were dramatically attenuated<sup>239</sup>, as would be predicted by a diminished  $\Sigma V$ . Moreover, when cocaine self-administration was reinstated in these rats (increasing  $\Sigma V$ ), the dopamine transients reappeared<sup>239</sup>.

The plasticity of the dopamine learning signal was explicitly evaluated in a set of experiments by Day and colleagues<sup>240</sup>. First, dopamine transients were detected at the unexpected presentation of a sucrose reward ( $\Sigma V = 0$ ), while a multimodal stimulus (light and lever extension) that did not predict anything did not evoke changes in dopamine concentration. In another group of rats, the multimodal stimulus (CS) had been repeatedly paired with the sucrose reward for several days. In this case, dopamine transients were detected at the presentation of the CS and not at the subsequent presentation of the sucrose ( $\Sigma V = \lambda$ , Figure 11). This shift in dopamine signal from the primary reward to the CS after learning confirms chemically what had previously been reported for dopamine cell firing<sup>206,233</sup>. Finally, Day and colleagues<sup>240</sup> examined the plasticity of the dopamine response during the early learning of the CS-US association. Rats received 25 pairings of the multimodal stimulus with sucrose. Dopamine transients occurred at the presentation of the sucrose during all of the pairings (Figure 11), with the peak of the dopamine signal time-locked to the retrieval of the sucrose pellet. In contrast, no changes in dopamine concentration were observed at the presentation of the CS during early pairings ( $\Sigma V = 0$ ), but in 4 out of 6 rats, dopamine transients emerged at the presentation of the CS later in the session, as learning occurred (as  $\Sigma V$  increased). Thus, these data provide evidence that dopamine transients are involved in learning about rewards and actively adapt during the learning process.

The hypothesis that fast dopamine signaling acts as a prediction error is focused on learning about CS-US associations. What does the animal do with this prediction error? Broadly speaking, dopamine transmission is thought to facilitate appetitive and seeking behavior<sup>241,242</sup>. Thus, dopamine transients that are triggered by rewards or stimuli that predict rewards could lead the animal to approach and consume the reward. Consistent with this, when behaviors were examined in the seconds immediately preceding and following dopamine transients during interaction with another rat, we found that while no particular behavior was always associated with the signals, transients were likely to be followed by approach behaviors to the other rat<sup>243</sup>. Further support comes from measurements of dopamine release during operant responding for sucrose<sup>244</sup>. In this study, a multimodal cue (light and lever extension) signaled sucrose availability. Remarkably, dopamine concentrations began to rise at the presentation of the cue, then peaked when the rat subsequently pressed the lever, suggesting that the dopamine transient induced by the CS facilitated the drive to obtain the sucrose. These and other data<sup>238</sup> suggest that dopamine transients can facilitate reward-seeking behavior.

If dopamine transients act as learning signals and direct subsequent behavior, what happens when phasic dopamine signaling becomes abnormal due to drugs or disease? In the case of a drug addiction, such dysfunction would presumably lead to abnormal learning and prediction errors that could underlie the pathological compulsion to seek and consume drugs. Moreover, the dopamine signals at the unexpected presentation of environmental cues previously associated with drug-taking may precipitate craving and relapse. Therefore, one potential target for pharmacological treatment of addiction may be the phasic dopamine signaling associated with addictive drugs. One potential therapeutic drug is rimonabant, a cannabinoid CB1 antagonist. In a recent voltammetric study, many acute effects of cocaine, nicotine and ethanol (including increased frequency of transients) were blocked by pretreatment with rimonabant<sup>224</sup>. As many anti-addiction medications are hypothesized to act on the positive reinforcing effects of drugs via the dopamine system, future research can use electrochemical techniques to directly test these hypotheses.



## 9. Electrophysiological tools to study the actions of neurotransmitters

Neuroscientists have developed a number of tools and approaches to study phenomena associated with neurotransmission. These include methods to record the electrical activity of neurons and methods to introduce minute amounts of chemical substances directly onto neurons. These are reviewed here because they are readily combined with the electrochemical sensors described in the previous sections. In addition, we review the systems in which dopamine effects have been studied. These vary greatly in complexity, and range from single cultured neurons to neurons in awake and behaving animals. Future advances in the understanding of chemical neurotransmission will require the combined use of these approaches.

### 9.1. Methods to measure the electrical activity of neurons

Electrophysiological methods sample the electrical properties of neurons and provide the most rapid, direct measurement of the effect of a neurotransmitter upon a neuron. Intracellular methods require inserting an electrode into a cell and monitoring the cellular response to a perturbation. For example, a current can be applied to the cell membrane while the electrode monitors subsequent changes in voltage. Excitatory and inhibitory potentials are observed when ion channels open in response to receptor activation. Alternatively, a specific voltage can be clamped across the membrane while the electrode measures current changes, termed excitatory or inhibitory currents. Patch clamp electrophysiology involves attaching a capillary to the membrane to form a high resistance seal at which current and voltage clamp experiments are performed. When used with an array of well established ion channel blockers, patch clamp can be used to measure the activity of a subset of ion channels on a cell membrane. Such intracellular techniques are commonly used with cell culture or slice experiments where the neurons are readily accessible to the experimenter, but its use is feasible only in rare cases in an awake animal<sup>245</sup>.

For *in vivo* preparations, extracellular recordings are frequently performed where changes in potential caused by ion flow from an action potential are measured at a distance from the target neuron. The electrode is connected to a high impedance amplifier, and the transient voltage signals resulting from neuronal firing are recorded. This technique is referred to as single-unit recording. It is readily combined with cyclic voltammetry by the use of an electronically controlled switch<sup>246</sup>. During voltammetry, the electrode is connected to a current transducer, and during single-unit recording it is connected to a voltage measuring amplifier. Single units can be detected with the electrode as far away as 50  $\mu\text{m}$  from a neuronal cell body<sup>247</sup>. The voltage changes that are measured are on the order of 50  $\mu\text{V}$  and have a duration of 1 – 2 ms. The voltages are measured versus a reference electrode and are both high-and low-pass filtered to enhance signals in the 300–3000 Hz range.

### 9.2. Methods to introduce chemical agents

A variety of techniques allow introduction of selective chemical agents into the brain. The major techniques are systemic administration, microinjection, reverse dialysis and iontophoresis.

In systemic application, the compound is introduced to the entire preparation, either through injection into the blood stream for animal preparations or introduction to the bath solution for cell and slice preparations. Though relatively simple, systemic techniques have several limitations, particularly in *in vivo* experiments. Many compounds cannot be administered in this manner due to their inability to cross the blood-brain barrier. Moreover, the entire brain is affected by the injection, potentially convoluting local results with changes up or downstream in the neural circuitry. Finally, systemic applications are slow in comparison to

the transient nature of neuronal signaling, often requiring several minutes for onset to occur, and hours or even days for complete clearance.

Microinjection is the administration of small volumes of a drug solution directly into a specific brain region. Because this approach targets a subset of the brain and circumvents the blood/brain barrier, microinjection offers many advantages over systemic application. Microinjection has been used extensively by Gerhardt and coworkers to examine the rate of disappearance of neurotransmitters<sup>248</sup>. A technique related to microinjection is reverse dialysis with a microdialysis probe. A compound capable of crossing the dialysis membrane is added to the buffer and diffuses from the probe into the sampling region. Both techniques greatly improve the spatial resolution for drug application, but are still slow (occurring over minutes) in comparison to rapid dopamine signaling.

Another approach, iontophoresis, is used to apply local concentrations of a compound with a net ionic charge over a period of a few seconds using an applied current. While producing locally large concentrations, iontophoresis only ejects small quantities of ions and, thus, clearance by diffusion is rapid. The amount of a given compound ejected follows the equation:

$$M = n \frac{it}{zF} \quad (19)$$

where the amount ejected in moles,  $M$ , is proportional to the ratio of the ejection current ( $i$ ) and ejection time ( $t$ ) to the charge ( $z$ ) and Faraday's constant ( $F$ )<sup>249</sup>. This ratio is modified by  $n$ , the ejection efficiency coefficient, which is empirically derived and varies significantly between electrodes, thereby making the technique only quantitative if direct measurement of ejection from each iontophoresis barrel is obtained<sup>250</sup>. For this reason, iontophoresis in most applications is not quantitative.

Iontophoresis also suffers from several other disadvantages. The actual concentration ejected is unknown and discriminating between a cell that is unresponsive to the manipulation and an unsuccessful ejection is difficult<sup>251</sup>. Additionally, at large ejection currents iontophoresis may electrically influence the activity of a neuron, independent of the pharmacological action of the compound actually being ejected. This confound makes discrimination between excitation and disinhibition impossible<sup>252</sup>. However, pairing iontophoresis with a detection technique such as cyclic voltammetry allows for concentrations and confirmation of ejection to be obtained, circumventing some of the key disadvantages of the technique (Figure 12). This was done some time ago<sup>246</sup>, but only recently has its use become more common<sup>253</sup>.

### 9.3. Uses of chemical and electrical stimulation

All of the methods described in the preceding section can be used to stimulate neuronal tissue either at the level of nerve, terminals, cell bodies, or both. The most general approach is to use agents that directly depolarize the cell membrane such as elevated concentrations of potassium ions or the excitatory amino acid n-methyl-d-aspartate (NMDA). Application of  $K^+$  depolarizes the cell, forcing voltage-dependent ion channels to open and generate an action potential. NMDA activates excitatory ionotropic glutamate receptors known as NMDA receptors which depolarize the cell and generate an action potential.

Release of neurotransmitters is also commonly evoked by electrical stimulation as described in Section 7.2. This method has several advantages over chemical methods. First, selectivity can be obtained by stimulating specific neuronal pathways. Second, the stimulations can be

brief, and third, there is no concern about diffusion of chemical reagents. However, electrical stimulations force all neurons within the stimulated region to release neurotransmitter simultaneously, which may not be an appropriate model for physiological release events.

Because nerve terminals from a variety of neurons are interspersed, local stimulation will generate release of several neurotransmitters. For this reason the results from chemical or electrical stimulations at the cell body, termed remote stimulations, are often more easy to interpret. As described in previous sections, remote stimulation of dopamine neurons *in vivo* can produce short duration dopamine release events similar to physiological release events. Because the stimulation occurs far from the terminal region, only neurons that project from the stimulated region to the terminal field will release neurotransmitter. This gives remote methods greater selectivity, although co-stimulation of other neurons may still occur.

One example of the non-selective nature of stimulations was obtained in a study of electrically stimulated dopamine release<sup>254</sup>. Dopamine release was generated via electrical stimulation of dopamine axons in the medial forebrain bundle, and both dopamine release and changes in postsynaptic cell firing were simultaneously measured (Section 9.1). Inhibitions and excitations of cell firing were recorded in response to the stimulation that coincided with the lifetime of dopamine release. At recording sites of cells inhibited by the stimulation, systemic injection of the vesicular monoamine transporter blocker RO4-1284 abolished dopamine release but not the postsynaptic inhibition. In contrast, systemic administration of bicuculline, a GABA<sub>A</sub> antagonist, abolished the inhibition of cell firing. These findings led to the conclusion that the inhibitions were caused by stimulating parallel axons that release GABA in the nucleus accumbens, whereas electrically stimulated dopamine release did not primarily impact the measured postsynaptic neuronal activity. These findings reveal a deficiency in the specificity of electrical and chemical stimulation of dopamine neurons that can obscure dopamine's actions.

#### 9.4. Neuronal preparations

The most common preparations for *in vitro* experiments are neuronal cell cultures. Cultured neurons are ideal for the study of vesicular exocytosis, as the environment can be precisely controlled, facilitating intracellular recording techniques. Neurons isolated in cultures undergo adaptive changes and often form synapses with themselves, known as autapses. Co-culture with glia and other neurons may improve the similarity to *in vivo* preparations. Another commonly used approach is to use brain slices. In this preparation the results are affected by the thickness and direction in which the brain is sliced. The slices need to be thin (200–300 μm) to allow diffusion of glucose and oxygen into the inner regions of the slice. Coronal slices are produced by taking a slice in the medial/lateral plane from the top to the bottom of the brain. Coronal slices through brain regions supporting dopamine release do not contain whole dopamine neurons, but only the dopamine terminals and their targets, the cell bodies of medium spiny neurons. Nevertheless, the terminals still release dopamine upon chemical or electrical stimulation. Sagittal and horizontal slices can contain whole dopamine neurons along with medium spiny neurons; sagittal slices are vertical slices along the entire length of the brain, and horizontal slices encompass the entire length of the brain along the horizontal plane. However, all slice preparations differ from *in vivo* preparations due to a lack of neurotransmitter tone and incomplete neural circuits that may confound the results<sup>203</sup>.

Neurotransmission in the intact brain has been investigated in both anesthetized and freely moving animals. Chloral hydrate and urethane are commonly used as anesthetics, and chemical or electrical sensors are implanted into the brain regions of interest through small holes in the skull. Atlases of rodent brain have been published, and they reference the

location of different brain substructures relative to landmarks on the skull. During experiments under anesthesia, the animal is usually placed in a stereotaxic apparatus which holds the animal in place and allows the use of micromanipulators for precise positioning of electrodes. However, anesthesia can cause drastic changes in neural activity<sup>255</sup>. Although technically more difficult to perform, experiments in freely moving animals provide the most physiologically relevant data as the neurons have experienced the least change from normal conditions. For example, dopamine effects in these experiments occur within the context of proper neurotransmitter tone, neural circuitry and firing rates. Moreover, measurement in freely moving animals is the only method in which dopamine transmission can be directly correlated to behavior.

The selections of recording technique, animal model, and drug delivery method control what information regarding dopamine neurotransmission can be obtained. Each technique and model introduces its own set of experimental confounds that must be considered in interpretation of the results. Through analysis of the unique observations obtained from the various recording techniques and animal models, a view of dopamine neurotransmission can emerge.

## 10. Investigating dopamine's actions on neurons

As described in earlier sections, the characteristics of the spontaneous release of dopamine are being revealed, and the next step is to characterize the way in which dopamine interacts with downstream neurons to affect behavior. This characterization requires a view of the relevant biochemical signaling pathways including receptors and their influence on neuronal activity.

### 10.1. Neurotransmitter receptors

The class of neurotransmitter receptors known as ionotropic receptors produces immediate effects upon neurotransmitter binding because they function as voltage-gated ion channels. Medium spiny neurons are the major target of dopamine release in the brain and have a resting potential of around  $-85$  mV. Increasing the conductance of sodium channels through activation of ionotropic receptors shifts the membrane potential to more positive values and, thus, may trigger an action potential. Conversely, other neurotransmitter receptors serve as chloride channels which hyperpolarize the cell, thereby reducing the probability of action potential generation. Opening calcium channels modulates neurotransmitter release, as well as impacts protein phosphorylation within the cell. By measuring the conductances of these specific receptor-linked channels and their effects on membrane potentials, electrophysiologists can unravel the effects of neurotransmitters that interact with ionotropic receptors.

In contrast, all identified dopamine receptors belong to the class of receptors known as G-protein coupled receptors<sup>252</sup>. Unlike ionotropic receptors, the G-protein coupled receptors are not directly linked to ion channels; instead, G-protein coupled receptors modulate neuronal activity through interactions with a G-protein complex<sup>256</sup>. When activated by the binding of a neurotransmitter, the  $\alpha$  subunit dissociates from the  $\gamma$ ,  $\beta$  complex and the receptor. The  $\alpha$  subunit then interacts with other proteins within the neuron, triggering signaling cascades capable of producing a variety of effects from modulating ion channel conductance to regulating protein expression. Activation of G-protein coupled receptors can produce effects that last only milliseconds, or generate changes that persist for hours or longer. Through a combination of electrophysiological and molecular biological experiments, the complex effects of dopamine release are being characterized.

## 10.2. Dopamine receptors

Several dopamine receptors have been identified. The receptors currently known have been placed into two primary groups based upon pharmacological characterization: the D1 family, which includes D<sub>1</sub> and D<sub>5</sub> receptors, and the D2 family, populated by D<sub>2</sub>, D<sub>3</sub>, and D<sub>4</sub> receptors. The D<sub>1</sub>, D<sub>2</sub>, and D<sub>3</sub> receptors show high expression levels in the nucleus accumbens<sup>257</sup>.

Dopamine receptors have been found to interact with potassium, sodium, and calcium channels through adenylate cyclase, which converts ATP into the secondary messenger, cAMP<sup>258</sup>. Investigations of the specific signaling cascades involving D1 and D2 receptors have found that a key molecular target for postsynaptic dopamine receptor activation is the protein DARPP-32. The DARPP-32 protein contains multiple phosphorylation sites. Depending upon the sites phosphorylated, DARPP-32 is capable of interacting with various protein phosphatases involved in cascades required for signal amplification and integration<sup>259</sup>. Recent models employing current knowledge of signaling cascades from D1 receptor activation have shown that modulation of cAMP-dependent kinase and DARPP-32 persists for several hundred milliseconds longer than the duration of the receptor activation<sup>260</sup>. Genetically modified mice that lack the DARPP-32 protein display a decreased ability of dopamine to modulate ion channels and long-term neuronal activity<sup>261</sup>. These knockout mice have also displayed attenuated behavioral responses to several drugs of abuse, such as locomotion in response to cocaine or amphetamine administration<sup>261</sup>.

Because G-protein coupled receptor effects are mediated by second messengers, they occur on a slower timescale than ionotropic receptor effects<sup>262</sup>. This delay is compounded by the design of dopaminergic synapses in which dopamine receptors and transporters are located both inside and outside of the synapse<sup>263</sup>. The net result is that dopamine must diffuse a greater distance to reach its receptors in comparison to neurotransmitters such as glutamate whose action is restricted to the synaptic cleft. The extra-synaptic action of dopamine has led to the label “volume” transmitter, and dopamine release events are believed to affect multiple targets<sup>186,264</sup>. A key example of dopamine’s delay was shown with observation of two distinct responses to dopamine neuron stimulation in anesthetized rats<sup>265</sup>. A rapid-onset excitation was followed by a second delayed excitation lasting several seconds after electrical stimulation of the medial forebrain bundle. The initial excitation was due to co-stimulation of glutamatergic neurons, while the delayed onset signal was found to be due to dopamine release. The experiments estimated that dopamine receptor effects upon neuronal activity have a delay of at least 200 ms from the release event until effects are observed<sup>265</sup>.

## 10.3. Presynaptic effects

Dopamine receptors are also located on the pre-synaptic terminals of dopamine neurons. Through these receptors, termed autoreceptors, dopamine can modulate subsequent release events (Section 7.2). Auto-inhibition of dopamine release is primarily mediated by D2 receptors. When dopamine is released, activation of pre-synaptic D2 receptors triggers an intracellular cascade of events that leads to a decrease in calcium channel conductance and down-regulation of tyrosine hydroxylase, an enzyme necessary for dopamine synthesis<sup>266-269</sup>.

Experiments characterizing autoreceptor function have been performed in rat brain slices and anesthetized rats using amperometry to detect dopamine release from a pair of electrical stimulus trains with differing separations between each stimulation<sup>203,205,270</sup>. Comparison of the relative maximum release from each stimulation allowed characterization of the timescale of D2 receptor effects. The data described the modulation of dopamine release with sub-second resolution over a time window of 200 ms to 5 s, with maximal inhibition at

700ms in slices. In the anesthetized experiment, a maximal inhibition between 150–300 ms after the stimulation was observed, with the effect disappearing within 600 ms. Moreover, as described above (Section 7.2), these inhibitory effects of D2 receptor activation on subsequent dopamine release desensitize over several seconds<sup>204</sup>.

Other neurotransmitters can also modulate release from dopaminergic nerve terminals. Experiments in cultured neurons, slices, and anesthetized animals have shown that dopamine release is strongly inhibited by increased glutamate levels<sup>271–273</sup>. Some controversy exists over the glutamate receptor responsible for the inhibition, with both mGluR5 and a signaling cascade involving AMPA receptors implicated<sup>235,236</sup>. The AMPA (alpha-amino-3-hydroxy-5-methyl-4-isoxazolepropionic acid) receptor cascade involves production of hydrogen peroxide which then modulates potassium channel conductance, decreasing dopamine release<sup>236</sup>. The mechanism involved in mGluR5-dependent inhibition has not yet been explored. Nevertheless, the experiments are all evidence for the influence of tonic glutamate levels upon dopamine release. Previous experiments have shown long-duration (30 minutes) dopamine concentrations increases in response to stimulation of the basolateral amygdala<sup>274,275</sup>. The increase in dopamine occurred with deactivation of the ventral tegmental area suggesting that the basolateral amygdala stimulation was generating release events at the terminals.

The modulation of dopamine release in the nucleus accumbens by nicotine, which activates nicotinic acetylcholine receptors, has also been observed<sup>276,277</sup>. Like glutamate, the application of nicotine inhibited dopamine release generated by a single release event. However, in experiments designed similar to the paired-pulse experiments described earlier involving D2 autoreceptors, nicotine was found to significantly increase the dopamine release evoked by the second pulse. This finding suggests a potential mechanism for acetylcholine's role in reward-based learning and nicotine use by enhancing dopamine release in response to repeated firing.

#### 10.4. Postsynaptic effects

Dopamine is released onto medium spiny neurons throughout the striatum. These neurons also receive glutamatergic input originating from the hippocampus, amygdala, prefrontal cortex and thalamus<sup>263,278</sup>. The current hypothesis for the role of dopamine is that it gates these incoming glutamatergic signals<sup>279</sup>. Specifically, dopamine is postulated to act as a filter to increase the “signal-to-noise” of a given target neuron's activity<sup>280</sup>. The local anatomy within the NAc supports this model, as dopamine terminals converge onto necks of dendritic spines and glutamatergic terminals project onto heads of the spines (Figure 13). As discussed previously, the extrasynaptic placement of dopamine receptors, coupled with volume transmission, allows dopamine to act across numerous targets. Dopamine release would therefore saturate the region surrounding the release site with relatively slow onset and offset and modulate the neuron's response to glutamatergic inputs.

Intracellular electrophysiological recordings in anesthetized rats have shown the existence of up and down states in medium spiny neurons<sup>281</sup>. The medium spiny neurons are dormant in the more negative down state at approximately  $-85$  mV, but they depolarize to approximately  $-55$  mV when entering the up state. Once in the up state, the neuron more readily generates action potentials in response to glutamatergic inputs. The driving force behind neurons entering the up state appears to be glutamate<sup>282</sup>. Dopamine finely tunes neuronal activity within the states by means of opposing effects from D1 and D2 receptors<sup>283</sup>. The activation of D1 receptors increases the conductance of L-type calcium channels and NMDA receptors, which stabilize the neuron in the up state<sup>284–286</sup>, leading to enhanced excitability of the medium spiny neurons. Alternatively, activation of postsynaptic D2 receptors reduces the conductance of calcium channels and excitatory AMPA receptors,

thereby reducing medium spiny neuron excitability<sup>285,287</sup>. Recent experiments<sup>245</sup> using intracellular recordings in awake rats found that medium spiny neurons displayed the predicted two-state behavior observed in slice preparations and anesthetized or asleep rats. However, the neurons exhibited only a single state – the up state – when rats were awake. This result calls into question the relevance of the up- and down-state hypothesis to interpret neural activity during behavior.

Extracellular recordings (which are unable to distinguish up and down states) in anesthetized and freely moving animals have primarily shown postsynaptic inhibitions in response to dopamine in spontaneously active and glutamate-excited cells<sup>258</sup>. Dopamine and amphetamine ejection via iontophoresis produced inhibitions that were blocked by both D1 and D2 antagonists<sup>288</sup>. However, stimulation of dopamine neurons has also been shown to produce notable excitatory effects from dopamine release. Postsynaptic excitations induced by NMDA injection into the medial forebrain bundle (which generates dopamine release) lasted for 1 s after the stimulation and were sensitive to D1 receptor activation and antagonism<sup>289</sup>.

Another example of the differential nature of dopamine's effects was observed in a study by Williams and Millar. These authors used voltammetric recordings to correlate dopamine release evoked by various electrical stimulus trains with changes in medium spiny neuron activity<sup>247</sup>. Medium spiny neurons displayed an increase in neuronal firing rate in response to nanomolar concentrations of dopamine release, but a decrease following release events producing more than 1  $\mu$ M dopamine. Both responses to dopamine were abolished by administration of alpha-methyl-*p*-tyrosine, which blocks dopamine synthesis and, thus, abolishes vesicular dopamine release. The experiment was later successfully replicated using introduction of dopamine via iontophoresis<sup>290</sup>. Although both D1 and D2 receptors were speculated to be responsible for these effects, pharmacological verification was not attempted.

The complex effects of dopamine on medium spiny neurons was elegantly explored in experiments by Sulzer and colleagues that addressed the convergence of dopamine and glutamate onto medium spiny neurons<sup>291</sup>. In the mouse slice, vesicular glutamate release was visualized with 2-photon microscopy, dopamine release was monitored with amperometry and FSCV, and postsynaptic changes in current were measured with whole-cell patch clamp recordings. These experiments revealed that, in addition to any direct effects on medium spiny neurons, dopamine modulated glutamate release onto these same neurons via D2 receptors. Interestingly, while the most active glutamatergic terminals appeared unaffected by D2 receptor activation, the other terminals were inhibited. Furthermore, dopamine input performed as a low pass filter, as the D2-mediated inhibition targeted glutamatergic terminals that had a low probability of release (i.e., released vesicles more slowly) and that were firing at high frequencies ( $\geq 10$  Hz). Therefore, by filtering less active glutamatergic inputs to the medium spiny neurons, dopamine amplifies only the most vigorous inputs.

Although the above experiments provide supporting evidence to elucidate the physiological actions of dopamine, they do not reveal the function of dopamine in mediating complex behavior tasks. For this goal, the spontaneous release of dopamine must be measured in real time and correlated to cell firing in freely moving animals. This was recently accomplished by using FSCV and electrophysiology at the same carbon-fiber electrode in rats<sup>253</sup>. The rats were trained to press a lever to receive a small stimulation train into the ventral tegmental area (i.e., intracranial self-stimulation), while neural activity was monitored in a subregion of the nucleus accumbens called the shell. Dopamine release was evoked in the nucleus accumbens by the electrical stimulation, but correlating dopamine release and neuronal cell

firing at the stimulation would incur confounds observed in previous studies<sup>254</sup> (see Section 9.3). Instead, *naturally occurring* dopamine release was correlated to cell firing. To reliably elicit a dopamine transient, a compound cue (tone and light) preceded the opportunity to press the lever by one second. As this cue consistently predicted the lever ( $\Sigma V = \lambda$ ), dopamine release was observed at the presentation of the cue (Figure 14). In addition, firing rates of the majority of medium spiny neurons examined significantly changed at the presentation of the cue as well. The most common response was an inhibition of firing (Figure 15), and the second most frequent response was an excitation in firing rate at the cue. Moreover, at almost 90% of the recording sites of these responsive medium spiny neurons, dopamine transients were observed as well. In contrast, at recording sites where neurons exhibited no change in firing at the cue, dopamine transients were typically absent, despite the presence of electrically evoked dopamine release (indicating the proximity of functional dopamine terminals). These data clearly demonstrate a correlation between naturally occurring dopamine transients and changes in postsynaptic firing rate<sup>254</sup>.

Pharmacological manipulations were further used to explore the functional role of these neural signals. First, dopamine receptor antagonists were microinjected into the accumbens shell and opposing D1/D2 effects were observed. While the D1 receptor antagonist blocked intracranial self-stimulation behavior at doses that did not affect general locomotion, a D2 receptor antagonist had no effect on intracranial self-stimulation behavior despite decreased locomotor activity. Second, dopamine receptor antagonists were iontophoretically applied to the accumbens shell adjacent to the carbon-fiber electrode to observe effects on firing patterns of medium spiny neurons. While the D2 receptor antagonist had no effect on cell firing, the D1 antagonist dramatically reduced both discrete inhibitions at the cue as well as overall firing rate. Although dopamine transients were not measured during iontophoretic application of the drugs, these data demonstrate that the association between dopamine transients and short-term changes in firing of medium spiny neurons is mediated by D1 receptors<sup>254</sup>.

### 10.5. Other neurotransmitters

Emerging evidence suggests that dopamine terminals may co-release glutamate in addition to dopamine. Currently, the expression of one type of vesicular glutamate transporter, the VGlut2, has been shown in neurons that stain positive for tyrosine hydroxylase<sup>292,293</sup>. The transporter is only expressed in a subset of DA neurons, and the majority of synapses formed by these neurons do not display morphology typical of glutamatergic synapses<sup>294</sup>. Robust expression of VGlut3, another vesicular glutamate transporter, has been shown in the striatum and accumbens<sup>295</sup>. The expression of another glutamate transporter, VGlut3, in serotonin, acetylcholine, and GABA neurons has been observed in other brain regions, though not in tyrosine hydroxylase-positive neurons at this time<sup>295,296</sup>.

Indirect electrophysiological evidence exists in cultured neurons and slices to support co-release of dopamine and glutamate. Investigation of dopamine neuron autapses, which are formed when a neuron forms a synapse with itself in culture, demonstrated excitatory postsynaptic potentials that were blocked by NMDA receptor antagonists in addition to dopamine receptor antagonists<sup>297</sup>. In brain slices, rapid and delayed-onset excitatory postsynaptic currents have been observed in response to dopamine neuron stimulation. In this experiment only the rapid onset signal was sensitive to an AMPA glutamate receptor antagonist<sup>298</sup>, indicating that this signal component resulted from glutamate release. Correcting for potential confounds such as co-release of other neurotransmitters requires full pharmacological analysis of post-synaptic effects. Thus, it is important to note that some studies, such as those by Gonon on the time course of postsynaptic effects of dopamine<sup>265</sup> (see Section 10.2), may have been confounded by co-release of glutamate.



The possibility of co-release of glutamate and dopamine provides a future challenge for investigators using *in vivo* chemical sensors of neurotransmitters. Simultaneous measurements of glutamate and dopamine with a combined microprobe, such as the multisided electrodes fabricated by Gerhardt<sup>89</sup>, could answer this question directly.

## 11. Investigating rapid changes in amino acid neurotransmitters

The electrochemically based sensors described in Section 6.2 are just beginning to be used in neurochemical applications. Their future use in behavioral experiments will undoubtedly lead to an increased understanding of their roles in behavior as is being discovered for dopamine. However, rapid microdialysis methods for amino acids have already reached a stage in development where they are providing important information on fast neurotransmitter changes during behavior. These approaches employ a conventional microdialysis probe but couple it online to a rapid separation system. This approach allows immediate analysis with complete separation times of less than a minute.

### 11.1. Rapid analysis of amines by capillary electrophoresis

To achieve fast sampling and analysis, rapid microdialysis systems employ online derivatization coupled with a gating approach that allows injection onto a fast separation scheme. For fluorescence analysis, two derivatizing agents have been employed. Naphthalene-2,3-dicarboxaldehyde has been used for the derivatization of dopamine and amino acids<sup>299</sup>, and *o*-phthalaldehyde has been used for derivatization of amines and amino acids<sup>300</sup>. The advantage of both of these reagents is that they do not fluoresce before derivatization but produce highly fluorescent derivatives of the neurotransmitter candidates. Following gated introduction into a capillary, the compounds are separated by capillary electrophoresis and detected by their fluorescence. Capillary electrophoresis requires low sample volumes, and so it is ideal for this application. Laser-induced fluorescence provides sensitivity in the attomole range. For amino acid separations, the separation can be repeated every 14 s, leading to high sample throughput and high temporal resolution to monitor chemical changes of neurotransmitters. With careful calibration of the dead time of the system, the timing of behavioral events can be associated with neurochemical changes. While the temporal resolution is not as high as with electrochemical sensors, the real advantage is that multiple compounds can be followed. Indeed, in one recent example, 62 distinct compounds could be monitored in less than one minute<sup>301</sup>.

### 11.2. Neurochemical studies with rapid microdialysis

Early applications of rapid microdialysis employed pharmacological agents<sup>299</sup> or depolarization with high K<sup>+</sup> solutions. For example, 60 mM K<sup>+</sup> was found to elevate glutamate, GABA, and taurine in the retina of the isolated larval salamander<sup>302</sup>. Similarly, D-serine release evoked by high K<sup>+</sup> in the rat striatum was monitored with 12.5 s resolution<sup>303</sup>. The time course of elevation of dopamine in the rat striatum following cocaine injection was followed with 2 minute resolution<sup>304</sup>. The entire time course could be followed for 16 min. In contrast, when dopamine was sampled by FSCV in a similar experiment, the tonic dopamine response to cocaine could only be followed for 2 min because of the inherent drift in the voltammetry experiment<sup>218</sup>. These two different approaches to the same experiment demonstrate the strengths and limitations of each technique.

Rapid microdialysis has been adapted for use in freely moving rats. This allows neurotransmitters to be monitored during behavior. Neurotransmitters were evaluated in the rat nucleus accumbens during exposure to the predator fox odor, 2, 5-dihydro-2,4,5-trimethylthiazoline<sup>305</sup>. Such odors elicit defensive behavioral responses in rats, such as increases in locomotion and burrowing. In rats that exhibited such behavior, enhanced

concentrations of glutamate and GABA were observed. However, animals that did not show such behavioral responses did not have a change in their striatal amino acid levels. The high temporal resolution revealed that the neurochemical changes were secondary to the behavioral changes. Thus, the neurochemical changes may have reflected the state of fear in the animal during exposure to the odorant.

Amino acids neurotransmitters have been measured during conditioned fear<sup>26</sup> in the amygdala, a brain area important for fearful emotion and memory. In this experiment, one set of rats were subjected to foot shock (US), while another group was exposed to a noise (CS) that preceded foot shock. During training, rapid and transient glutamate and GABA concentration increases were observed during the first pairing of the CS and US. In contrast, rats receiving un signaled shock showed few changes at first, but with continued shocks glutamate tended to increase. These chemical changes occurred on a subminute time scale and would have been difficult to distinguish with slower sampling.

### 11.3. Current advances in rapid microdialysis

As the previous examples show, rapid microdialysis is a very powerful technique that provides multicomponent analyses on a time scale that is compatible with many neurochemical processes. However, assembling and miniaturizing all of the necessary components has restricted its use. Two approaches are directed at making its use more commonplace. First is the use of microfluidic chips to allow the derivatization, gated introduction, separation and detection all on one chip<sup>306</sup>. Early developments in this regard show that sensitivity can be maintained while the operation is simplified and automated. The second development is the use of miniaturized sampling devices that lessen the damage to tissue caused by the microdialysis probes in use today<sup>307,308</sup>. These developments will expand the use of this promising technique.

## 12. Conclusions

Investigating the role of neurotransmitters on neural activity and animal behavior is a complex task, but improvement of detection techniques makes real-time measurement of physiological concentrations of some neurotransmitters in the brain possible. To form a complete view of chemical neurotransmission, the interaction between factors modulating release, post-synaptic firing rates, and intracellular signaling need to be investigated. A wealth of information regarding the actions of dopamine in cultured cells, brain slices, and anesthetized animals has been produced to date. A current advance is correlation of real-time presynaptic dopamine release events with postsynaptic cell firing in awake, behaving animals. In such a complex system, the potential for non-dopaminergic effects convoluting the interpretation of results is high. Thus, it will be important to pair the recording techniques with local drug delivery systems such as iontophoresis to confirm dopamine's actions. Although the technology is currently in place to achieve this goal for dopamine neurotransmission, the development of newer sensors will enable this concept to be extended to a larger number of neurotransmitters. Future directions for innovation include sensor arrays, electrodes that can be chronically implanted, and the combined use of sensors and other traditional approaches to gain a more complete understanding of chemical neurotransmission.

## Acknowledgments

Research in the Wightman laboratory on this topic has been supported by NIH.

## Abbreviations

<b>AMPA</b>	$\alpha$ -amino-3-hydroxy-5-methyl-4-isoxazolepropionic acid; a glutamate analog that activates the ionotropic AMPA receptor for glutamate
<b>CS</b>	Conditioned stimulus; a previously neutral stimulus that gains significance as it is repeatedly paired with an unconditioned stimulus
<b>DOPAC</b>	3,4 dihydroxyphenylacetic acid
<b>fMRI</b>	Functional magnetic resonance imaging; a spectroscopic technique
<b>FSCV</b>	Fast-scan cyclic voltammetry
<b>GABA</b>	$\gamma$ -aminobutyric acid
<b>L-DOPA</b>	3,4-dihydroxyphenylalanine
<b>NMDA</b>	N-methyl-d-aspartate; an amino acid derivative that activates the ionotropic NMDA receptor for glutamate
<b>PET</b>	Positron emission tomography; a spectroscopic technique
<b>US</b>	Unconditioned stimulus; a stimulus that evokes an innate response, such as a food or drug reward
<b><math>\lambda - \Sigma V</math></b>	prediction error in learning model, with $\lambda$ as the maximum amount of learning or prediction that can be achieved of the predictability of the US, and $\Sigma V$ as the sum of the amount of learning (or prediction) that actually occurred at a given presentation of the US

## References

1. Wise RA. Drug Alcohol Depend. 1998; 51:13. [PubMed: 9716927]
2. Berridge KC, Robinson TE. Brain Res. Brain Res. Rev. 1998; 28:309. [PubMed: 9858756]
3. Tobler PN, Fiorillo CD, Schultz W. Science. 2005; 307:1642. [PubMed: 15761155]
4. Pan WX, Schmidt R, Wickens JR, Hyland BI. J. Neurosci. 2005; 25:6235. [PubMed: 15987953]
5. Kandel, ER. Search of Memory. 1st ed.. New York, NY: W. W. Norton and Company, Inc.; 2006.
6. Deadwyler SA, Hampson RE. Behav. Brain Res. 2006
7. Chapin JK, Nicolelis MA. J Neurosci. Methods. 1999; 94:121. [PubMed: 10638820]
8. Eccles JC, Jaeger JC. Proc. Roy. Soc. 1958; 148B:38.
9. Douglas WW. Br. J. Pharmacol. 1968; 34:453.
10. Valtorta F, Fesce R, Grohovaz F, Haimann C, Hurlbut WP, Iezzi N, Torri Tarelli F, Villa A, Ceccarelli B. Neurosci. 1990; 35:477.
11. Wightman RM, Jankowski JA, Kennedy RT, Kawagoe KT, Schroeder TJ, Leszczyszyn DJ, Near JA, Diliberto EJ Jr. Viveros OH. Proc. Natl. Acad. Sci. U.S.A. 1991; 88:10754. [PubMed: 1961743]
12. Pothos EN, Przedborski S, Davila V, Schmitz Y, Sulzer D. J. Neurosci. 1998; 18:5575. [PubMed: 9671649]
13. Staal RGW, Mosharov EV, Sulzer D. Nature Neurosci. 2004; 7:341. [PubMed: 14990933]
14. Hochstetler SE, Puopolo M, Gustincich S, Raviola E, Wightman RM. Anal. Chem. 2000; 72:489. [PubMed: 10695133]
15. Amatore C, Arbault S, Guille M, Lemaitre F. Chemphyschem. 2007
16. Watson CJ, Venton BJ, Kennedy RT. Anal. Chem. 2006; 78:1391. [PubMed: 16570388]
17. Justice JB Jr. J. Neurosci. Methods. 1993; 48:263. [PubMed: 8105154]
18. Olson RJ, Justice JB Jr. Anal. Chem. 1993; 65:1017. [PubMed: 8494171]
19. Lu Y, Peters JL, Michael AC. J. Neurochem. 1998; 70:584. [PubMed: 9453552]

20. Bungay PM, Newton-Vinson P, Isele W, Garris PA, Justice JB. *J. Neurochem.* 2003; 86:932. [PubMed: 12887691]
21. Yang H, Peters JL, Allen C, Chern SS, Coalson RD, Michael AC. *Anal. Chem.* 2000; 72:2042. [PubMed: 10815963]
22. Clapp-Lilly KL, Roberts RC, Duffy LK, Irons KP, Hu Y, Drew KL. *J. Neurosci. Methods.* 1999; 90:129. [PubMed: 10513596]
23. Cheng J, Feenstra MG. *Learn. Mem.* 2006; 13:168. [PubMed: 16585792]
24. Lorrain DS, Riolo JV, Matuszewich L, Hull EM. *J. Neurosci.* 1999; 19:7648. [PubMed: 10460270]
25. Young AM. *J. Neurosci. Methods.* 2004; 138:57. [PubMed: 15325112]
26. Venton BJ, Robinson TE, Kennedy RT, Maren S. *Eur. J. Neurosci.* 2006; 23:3391. [PubMed: 16820029]
27. Volkow ND, Wang GJ, Ma Y, Fowler JS, Wong C, Ding YS, Hitzemann R, Swanson JM, Kalivas P. *J. Neurosci.* 2005; 25:3932. [PubMed: 15829645]
28. Knutson B, Fong GW, Bennett SM, Adams CM, Hommer D. *Neuroimage.* 2003; 18:263. [PubMed: 12595181]
29. Peters JL, Miner LH, Michael AC, Sesack SR. *J. Neurosci. Methods.* 2004; 137:9. [PubMed: 15196823]
30. Kissinger PT, Hart JB, Adams RN. *Brain Res.* 1973; 55:209. [PubMed: 4145914]
31. Adams RN. *Prog. Neurobiol.* 1990; 35:297. [PubMed: 1980746]
32. Adams RN, Marsden CA. *Handb. Psychopharmacol.* 1982; 15:1.
33. Hummon AB, Amare A, Sweedler JV. *Mass. Spectrom. Rev.* 2006; 25:77. [PubMed: 15937922]
34. Haskins WE, Watson CJ, Cellar NA, Powell DH, Kennedy RT. *Anal. Chem.* 2004; 76:5523. [PubMed: 15362916]
35. Fu Q, Tang LS, Marder E, Li L. *J. Neurochem.* 2007; 101:1099. [PubMed: 17394556]
36. Adams, RN.; Marsden, CA. *Handbook of Psychopharmacology.* Iversen, LL.; Iversen, SD.; Snyder, SH., editors. Vol. Vol. 15. New York: Plenum Press; 1982.
37. Cooper, JR.; Bloom, FE.; Roth, RH., editors. *The Biochemical Basis of Neuropharmacology.* Eighth Edition. 2003.
38. Hawley MD, Tatawawadi SV, Piekarski S, Adams RN. *J. Am. Chem. Soc.* 1967; 89:447. [PubMed: 6031636]
39. Blank CL, McCreery RL, Wightman RM, Chey W, Adams RN, Reid JR, Smismann EE. *J. Med. Chem.* 1976; 19:178. [PubMed: 1246041]
40. Zhang F, Dryhurst G. *Bioorganic Chem.* 1993; 21:392.
41. Ciolkowski EL, Cooper BR, Jankowski JA, Jorgenson JW, Wightman RM. *J. Am. Chem. Soc.* 1992; 114:2815.
42. Pihel K, Schroeder TJ, Wightman RM. *Anal. Chem.* 1994; 66:4532.
43. Wrona MZ, Dryhurst G. *Bioorganic Chem.* 1990; 18:291.
44. Pihel K, Hsieh S, Jorgenson JW, Wightman RM. *Anal. Chem.* 1995; 67:4514. [PubMed: 8633786]
45. Abou El-Nour K, Brajter-Toth A. *Analyst.* 2003; 128:1056. [PubMed: 12964607]
46. Brajter-Toth A, Abou El-Nour K, Cavalheiro ET, Bravo R. *Anal. Chem.* 2000; 72:1576. [PubMed: 10763255]
47. Abou El-Nour K, Brajter-Toth A. *Electroanal.* 2000; 12:805.
48. Swamy BEK, Venton BJ. *Anal. Chem.* 2007; 79:744. [PubMed: 17222045]
49. Mefford IN, Oke AF, Adams RN. *Brain Res.* 1981; 212:223. [PubMed: 7225858]
50. Nagy G, Rice ME, Adams RN. *Life Sci.* 1982; 31:2611. [PubMed: 6130453]
51. Mueller K. *Pharmacol. Biochem. Behav.* 1986; 25:325. [PubMed: 3763657]
52. Gonon F, Buda M, Cespuglio R, Jouvet M, Pujol JF. *Nature.* 1980; 286:902. [PubMed: 7412872]
53. Gonon FG, Fombarlet CM, Buda MJ, Pujol JF. *Anal. Chem.* 1981; 53:1386.
54. Marsden CA, Joseph MH, Kruk ZL, Maidment NT, Oneill RD, Schenk JO, Stamford JA. *Neurosci.* 1988; 25:389.
55. Millar J, Oconnor JJ, Trout SJ, Kruk ZL. *J. Neurosci. Methods.* 1992; 43:109. [PubMed: 1405738]

56. Wiedemann DJ, Bassetomusk A, Wilson RL, Rebec GV, Wightman RM. *J. Neurosci. Methods.* 1990; 35:9. [PubMed: 2148961]
57. Baur JE, Kristensen EW, May LJ, Wiedemann DJ, Wightman RM. *Anal. Chem.* 1988; 60:1268. [PubMed: 3213946]
58. Sternson AW, McCreery R, Feinberg B, Adams RN. *J. Electroanal. Chem.* 1973; 46:313.
59. Chen BT, Avshalumov MV, Rice ME. *J. Neurophys.* 2001; 85:2468.
60. Avshalumov MV, Bao L, Patel JC, Rice ME. *Antioxidants Redox Signaling.* 2007; 9:219. [PubMed: 17115944]
61. Kulagina NV, Michael AC. *Anal. Chem.* 2003; 75:4875. [PubMed: 14674466]
62. Zimmerman JB, Wightman RM. *Anal. Chem.* 1991; 63:24. [PubMed: 1810167]
63. Bolger FB, Lowry JP. *Sensors.* 2005; 5:473.
64. Venton BJ, Michael DJ, Wightman RM. *J. Neurochem.* 2003; 84:373. [PubMed: 12558999]
65. Thompson JK, Peterson MR, Freeman RD. *Science.* 2003; 299:1070. [PubMed: 12586942]
66. Ogawa S, Lee TM, Kay AR, Tank DW. *Proc. Natl. Acad. Sci. U.S.A.* 1990; 87:9868. [PubMed: 2124706]
67. Schuman EM, Madison DV. *Ann. Rev. Neurosci.* 1994; 17:153. [PubMed: 7516125]
68. Dawson VL, Dawson TM. *Neurochem. Internat.* 1996; 29:97.
69. Wightman RM, Wipf DO. *Accounts. Chem. Res.* 1990; 23:64.
70. Kissinger PT, Hart JB, Adams RN. *Brain Res.* 1973; 55:209. [PubMed: 4145914]
71. Adams RN. *Anal. Chem.* 1958; 30:1576.
72. O'Neill RD. *Sensors.* 2005; 5:317.
73. O'Neill RD, Grunewald RA, Fillenz M, Albery WJ. *Neurosci.* 1982; 7:1945.
74. Conti JC, Strobe E, Adams RN, Marsden CA. *Life Sci.* 1978; 23:2705. [PubMed: 739848]
75. Huff RM, Adams RN. *Neuropharmacol.* 1980; 19:587.
76. Gonon F, Cespuglio R, Ponchon JL, Buda M, Jouvret M, Adams RN, Pujol JF. *C. R. Acad. Sci. Hebd. Seances. Acad. Sci. D.* 1978; 286:1203. [PubMed: 96981]
77. Ponchon JL, Cespuglio R, Gonon F, Jouvret M, Pujol JF. *Anal. Chem.* 1979; 51:1483. [PubMed: 484865]
78. McCreery, RL. *Laboratory Techniques in Electroanalytical Chemistry.* Vol. Chapter 10. New York: Dekker; 1996.
79. Kawagoe KT, Zimmerman JB, Wightman RM. *J. Neurosci. Methods.* 1993; 48:225. [PubMed: 8412305]
80. Chen P, McCreery RL. *Anal. Chem.* 1996; 68:3958.
81. Heien ML, Phillips PE, Stuber GD, Seipel AT, Wightman RM. *Analyst.* 2003; 128:1413. [PubMed: 14737224]
82. Kovach PM, Deakin MR, Wightman RM. *J. Phys. Chem.* 1986; 90:4612.
83. Swain GM, Kuwana T. *Analytical Chemistry.* 1991; 63:517.
84. Yan JL, Du Y, Liu JF, Cao WD, Sun SH, Zhou WH, Yang XR, Wang EK. *Anal. Chem.* 2003; 75:5406. [PubMed: 14710819]
85. Matos RC, Angnes L, Araujo MCU, Saldanha TCB. *Analyst.* 2000; 125:2011. [PubMed: 11193090]
86. Vandaveer WR, Woodward DJ, Fritsch I. *Electrochimica Acta.* 2003; 48:3341.
87. Etienne M, Oni J, Schulte A, Hartwich G, Schuhmann W. *Electrochimica Acta.* 2005; 50:5001.
88. Burmeister JJ, Moxon, Karen, Gerhardt, Greg A. *Anal. Chem.* 2000; 72:187. [PubMed: 10655652]
89. Burmeister JJ, Gerhardt GA. *Trends Anal. Chem.* 2003; 22:498.
90. Burmeister JJ, Gerhardt GA. *Anal. Chem.* 2001; 73:1037. [PubMed: 11289414]
91. Phillips PE, Robinson DL, Stuber GD, Carelli RM, Wightman RM. *Methods Mol. Med.* 2003; 79:443. [PubMed: 12506716]
92. Witkowski A, Brajtertoth A. *Anal. Chem.* 1992; 64:635. [PubMed: 1580361]
93. Hsueh CC, Brajtertoth A. *Anal. Chem.* 1994; 66:2458.

94. Pihel K, Walker QD, Wightman RM. *Anal. Chem.* 1996; 68:2084. [PubMed: 9027223]
95. Wang J, Pamidi PVA, Cepria G, Basak S, Rajeshwar K. *Analyst.* 1997; 122:981. [PubMed: 9374028]
96. Kawagoe KT, Wightman RM. *Talanta.* 1994; 41:865. [PubMed: 18966011]
97. Lyne PD, Oneill RD. *Anal. Chem.* 1989; 61:2323.
98. Lane RF, Blaha CD. *Langmuir.* 1990; 6:56.
99. Blaha CD, Phillips AG. *Behav. Pharmacol.* 1996; 7:675. [PubMed: 11224465]
100. Bath BD, Martin HB, Wightman RM, Anderson MR. *Langmuir.* 2001; 17:7032.
101. Downard AJ, Roddick AD, Bond AM. *Analytica Chimica Acta.* 1995; 317:303.
102. Hermans A, Seipel AT, Miller CE, Wightman RM. *Langmuir.* 2006; 22:1964. [PubMed: 16489775]
103. Shibuki K. *Neurosci. Res.* 1990; 9:69. [PubMed: 2175870]
104. Friedemann MN, Robinson SW, Gerhardt GA. *Anal. Chem.* 1996; 68:2621. [PubMed: 8694261]
105. Amatore C, Arbault S, Bouton C, Coffi K, Drapier JC, Ghandour H, Tong Y. *Chembiochem.* 2006; 7:653. [PubMed: 16502474]
106. Ichimori K, Ishida H, Fukahori M, Nakazawa H, Murakami E. *Rev. Scientific Instruments.* 1994; 65:2714.
107. Griveau S, Dumezy C, Seguin J, Chabot GG, Scherman D, Bedioui F. *Anal. Chem.* 2007; 79:1030. [PubMed: 17263331]
108. Isik S, Castillo J, Blochl A, Csoregi E, Schuhmann W. *Bioelectrochem.* 2007; 70:173.
109. Shin JH, Weinman SW, Schoenfisch MH. *Anal. Chem.* 2005; 77:3494. [PubMed: 15924380]
110. Leszczyszyn DJ, Jankowski JA, Viveros OH, Diliberto EJ, Near JA, Wightman RM. *J. Neurochem.* 1991; 56:1855. [PubMed: 2027003]
111. Zhou Z, Mislis S. *J. Biol. Chem.* 1995; 270:3498. [PubMed: 7876083]
112. Cahill PS, Wightman RM. *Anal. Chem.* 1995; 67:2599. [PubMed: 8849026]
113. Chen TK, Luo G, Ewing AG. *Anal. Chem.* 1994; 66:3031. [PubMed: 7978300]
114. Pothos EN, Davila V, Sulzer D. *J. Neurosci.* 1998; 18:4106. [PubMed: 9592091]
115. Jaffe EH, Marty A, Schulte A, Chow RH. *J. Neurosci.* 1998; 18:3548. [PubMed: 9570786]
116. Dugast C, Suaud-Chagny MF, Gonon F. *Neurosci.* 1994; 62:647.
117. Troyer KP, Heien MLAV, Venton BJ, Wightman RM. *Curr. Opinion Chem.Biol.* 2002; 6:696.
118. Venton BJ, Troyer KP, Wightman RM. *Anal. Chem.* 2002; 74:539. [PubMed: 11838672]
119. Daws LC, Montanez S, Owens WA, Gould GG, Frazer A, Toney GM, Gerhardt GA. *J. Neurosci. Methods.* 2005; 143:49. [PubMed: 15763136]
120. Perez XA, Andrews AM. *Anal. Chem.* 2005; 77:818. [PubMed: 15679349]
121. Hoffman AF, Gerhardt GA. *J. Neurochem.* 1998; 70:179. [PubMed: 9422361]
122. Miller AD, Forster GL, Yeomans JS, Blaha CD. *Neurosci.* 2005; 136:531.
123. Unger EL, Eve DJ, Perez XA, Reichenbach DK, Xu YQ, Lee MK, Andrews AM. *Neurobiol. Dis.* 2006; 21:431. [PubMed: 16230020]
124. Gonon FG, Navarre F, Buda MJ. *Anal. Chem.* 1984; 56:573. [PubMed: 6711824]
125. Crespi F, Paret J, Keane PE, Morre M. *Neurosci. Letters.* 1984; 52:159.
126. Millar J, Stamford JA, Kruk ZL, Wightman RM. *Eur. J. Pharmacol.* 1985; 109:341. [PubMed: 3872803]
127. Hsueh C, Bravo R, Jaramillo AJ, BrajterToth A. *Analytica Chimica Acta.* 1997; 349:67.
128. Howell JO, Kuhr WG, Ensman RE, Wightman RM. *J. Electroanal. Chem.* 1986; 209:77.
129. Cahill PS, Walker QD, Finnegan JM, Mickelson GE, TravisZ ER, Wightman RM. *Anal. Chem.* 1996; 68:3180. [PubMed: 8797378]
130. Heien ML, Johnson MA, Wightman RM. *Anal. Chem.* 2004; 76:5697. [PubMed: 15456288]
131. Bath BD, Michael DJ, Trafton BJ, Joseph JD, Runnels PL, Wightman RM. *Anal. Chem.* 2000; 72:5994. [PubMed: 11140768]
132. Michael D, Travis ER, Wightman RM. *Anal. Chem.* 1998; 70:586A.

133. Robinson DL, Venton BJ, Heien ML, Wightman RM. *Clin. Chem.* 2003; 49:1763. [PubMed: 14500617]
134. Kramer, R. *Chemometric Techniques for Quantitative Analysis*. New York: Marcel Dekker, Inc.; 1998.
135. Jackson JE, Mudholkar GS. *Technometrics*. 1979; 21:341.
136. Chesler M, Chan CY. *Neurosci.* 1988; 27:941.
137. Chesler M, Chen JCT, Kraig RP. *J. Neurosci. Methods*. 1994; 53:129. [PubMed: 7823615]
138. Chen JCT, Chesler M. *Proc. Nat. Aca. Sci. U. S. A.* 1992; 89:7786.
139. Marzouk SAM, Ufer S, Buck RP, Johnson TA, Dunlap LA, Cascio WE. *Anal. Chem.* 1998; 70:5054. [PubMed: 9852787]
140. Bezbaruah AN, Zhang TC. *Anal. Chem.* 2002; 74:5726. [PubMed: 12463355]
141. Johnson MD, Kao OE, Kipke DR. *J. Neurosci. Methods*. 2007; 160:276. [PubMed: 17084461]
142. Runnels PL, Joseph JD, Logman MJ, Wightman RM. *Anal. Chem.* 1999; 71:2782. [PubMed: 10424168]
143. Cheer JF, Wassum KM, Wightman RM. *J. Neurochem.* 2006; 97:1145. [PubMed: 16686693]
144. Llaudet E, Botting NP, Crayston JA, Dale N. *Biosens. Bioelectron.* 2003; 18:43. [PubMed: 12445443]
145. Dale N, Pearson T, Frenguelli BG. *J. Physiol. London.* 2000; 526:143. [PubMed: 10878107]
146. Wilson GS, Gifford R. *Biosens. Bioelectron.* 2005; 20:2388. [PubMed: 15854814]
147. Clark LC, Lyons C. *Ann. N. Y. Aca. Sci.* 1962; 102:29.
148. Updike SJ, Hicks GP. *Nature*. 1967; 214:986. [PubMed: 6055414]
149. Gregg BA, Heller A. *J. Phys. Chem.* 1991; 95:5976.
150. Georganopoulou DG, Carley R, Jones DA, Boutelle MG. *Faraday Disc.* 2000:291.
151. Wang J. *Electroanalysis*. 2001; 13:983.
152. Bindra DS, Zhang YN, Wilson GS, Sternberg R, Thevenot DR, Moatti D, Reach G. *Anal. Chem.* 1991; 63:1692. [PubMed: 1789439]
153. Hu YB, Wilson GS. *J. Neurochem.* 1997; 68:1745. [PubMed: 9084449]
154. Silver IA, Erecinska M. *J. Neurosci.* 1994; 14:5068. [PubMed: 8046468]
155. Hu YB, Wilson GS. *J. Neurochem.* 1997; 69:1484. [PubMed: 9326277]
156. Shram NF, Netchiporouk LI, Martelet C, Jaffrezic-Renault N, Bonnet C, Cespuoglio R. *Anal. Chem.* 1998; 70:2618. [PubMed: 9666730]
157. Shram N, Netchiporouk L, Cespuoglio R. *Eur. J. Neurosci.* 2002; 16:461. [PubMed: 12193189]
158. Wang DL, Heller A. *Anal. Chem.* 1993; 65:1069. [PubMed: 8494172]
159. Zimmerman JB, Wightman RM. *Anal. Chem.* 1991; 63:24. [PubMed: 1810167]
160. Parkin MC, Hopwood SE, Jones DA, Hashemi P, Landolt H, Fabricius M, Lauritzen M, Boutelle MG, Strong AJ. *J. Cereb. Blood Flow Metab.* 2005; 25:402. [PubMed: 15703701]
161. Jones DA, Ros J, Landolt H, Fillenz M, Boutelle MG. *J. Neurochem.* 2000; 75:1703. [PubMed: 10987853]
162. Alvarez-Crespo SL, Lobo-Castanon MJ, Miranda-Ordieres AJ, Tunon-Blanco P. *Biosens. Bioelectron.* 1997; 12:739. [PubMed: 9421885]
163. Kulagina NV, Shankar L, Michael AC. *Anal. Chem.* 1999; 71:5093. [PubMed: 10575963]
164. Pan ST, Arnold MA. *Talanta*. 1996; 43:1157. [PubMed: 18966594]
165. Huettl P, French K, Pomerleau FP, Palmer MR, Burmeister JJ, Granholm AC, Gerhardt GA. *Exp. Neurol.* 2002; 175:439.
166. Oldenzel WH, Dijkstra G, Cremers TIFH, Westerink BHC. *Anal. Chem.* 2006; 78:3366. [PubMed: 16689539]
167. Kusakabe H, Midorikawa Y, Fujishima T, Kuninaka A, Yoshino H. *Agri. Biol. Chem.* 1983; 47:1323.
168. Garguilo MG, Michael AC. *J. Am. Chem. Soc.* 1993; 115:12218.
169. Garguilo MG, Michael AC. *Anal. Chem.* 1994; 66:2621. [PubMed: 7943733]

170. Guerrieri A, Lattanzio V, Palmisano F, Zambonin PG. *Biosens. Bioelectron.* 2006; 21:1710. [PubMed: 16169212]
171. Garguilo MG, Michael AC. *J. Neurosc. Methods.* 1996; 70:73.
172. Xin Q, Wightman RM. *Brain Res.* 1997; 776:126. [PubMed: 9439804]
173. Mazzei F, Botre F, Lorenti G, Porcelli F. *Analytica Chimica Acta.* 1996; 328:41.
174. Llaudet E, Hatz S, Droniou M, Dale N. *Anal. Chem.* 2005; 77:3267. [PubMed: 15889918]
175. Llaudet E, Botting NP, Crayston JA, Dale N. *Biosens Bioelectron.* 2003; 18:43. [PubMed: 12445443]
176. Dale N, Hatz S, Tian F, Llaudet E. *Trends Biotechnol.* 2005; 23:420. [PubMed: 15950302]
177. Compagnone D, Guilbault GG. *Analytica Chimica Acta.* 1997; 340:109.
178. Kueng A, Kranz C, Mizaikoff B. *Biosens Bioelectron.* 2004; 19:1301. [PubMed: 15046763]
179. Murphy LJ, Galley PT. *Anal. Chem.* 1994; 66:4345. [PubMed: 7847632]
180. Nicholson C, Phillips JM. *J. Physiol.* 1981; 321:225. [PubMed: 7338810]
181. Kelly RS, Wightman RM. *Brain Res.* 1987; 423:79. [PubMed: 3676822]
182. Horn AS. *Prog. Neurobiol.* 1990; 34:387. [PubMed: 2192393]
183. Giros B, Jaber M, Jones SR, Wightman RM, Caron MG. *Nature.* 1996; 379:606. [PubMed: 8628395]
184. Nicholson C. *Biophys. J.* 1995; 68:1699. [PubMed: 7612814]
185. Cragg SJ, Rice ME. *Trends Neurosci.* 2004; 27:270. [PubMed: 15111009]
186. Venton BJ, Zhang H, Garris PA, Phillips PE, Sulzer D, Wightman RM. *J. Neurochem.* 2003; 87:1284. [PubMed: 14622108]
187. Garris PA, Wightman RM. *Synapse.* 1995; 20:269. [PubMed: 7570359]
188. Near JA, Bigelow JC, Wightman RM. *J. Pharmacol. Exp. Ther.* 1988; 245:921. [PubMed: 3385647]
189. Wightman RM, Amatore C, Engstrom RC, Hale PD, Kristensen EW, Kuhr WG, May LJ. *Neurosci.* 1988; 25:513.
190. Kristensen EW, Kuhr WG, Wightman RM. *Anal. Chem.* 1987; 59:1752. [PubMed: 3631500]
191. Wu Q, Reith ME, Walker QD, Kuhn CM, Carroll FI, Garris PA. *J. Neurosci.* 2002; 22:6272. [PubMed: 12122086]
192. Mitchell K, Oke AF, Adams RN. *J. Neurochem.* 1994; 63:917. [PubMed: 8051568]
193. Bunin MA, Wightman RM. *J. Neurosci.* 1998; 18:4854. [PubMed: 9634551]
194. Wu Q, Reith ME, Wightman RM, Kawagoe KT, Garris PA. *J. Neurosci. Methods.* 2001; 112:119. [PubMed: 11716947]
195. Ewing AG, Bigelow JC, Wightman RM. *Science.* 1983; 221:169. [PubMed: 6857277]
196. Michael AC, Ikeda M, Justice JB Jr. *Brain Res.* 1987; 421:325. [PubMed: 3500755]
197. Justice JB Jr, Nicolaysen LC, Michael AC. *J. Neurosci. Meth.* 1988; 22:239.
198. Venton BJ, Seipel AT, Phillips PE, Wetsel WC, Gitler D, Greengard P, Augustine GJ, Wightman RM. *J. Neurosci.* 2006; 26:3206. [PubMed: 16554471]
199. Pieribone VA, Shupliakov O, Brodin L, Hilfiker-Rothenfluh S, Czernik AJ, Greengard P. *Nature.* 1995; 375:493. [PubMed: 7777058]
200. Garris PA, Kilpatrick M, Bunin MA, Michael D, Walker QD, Wightman RM. *Nature.* 1999; 398:67. [PubMed: 10078530]
201. Montague PR, McClure SM, Baldwin PR, Phillips PE, Budygin EA, Stuber GD, Kilpatrick MR, Wightman RM. *J. Neurosci.* 2004; 24:1754. [PubMed: 14973252]
202. Yavich L, MacDonald E. *Brain Res.* 2000; 870:73. [PubMed: 10869503]
203. Phillips PE, Hancock PJ, Stamford JA. *Synapse.* 2002; 44:15. [PubMed: 11842442]
204. Kita JM, Parker LE, Phillips PEM, Garris PA, Wightman RM. *J. Neurochem.* 2007 *in press.*
205. Kennedy RT, Jones SR, Wightman RM. *J. Neurochem.* 1992; 59:449. [PubMed: 1352798]
206. Schultz W, Dayan P, Montague PR. *Science.* 1997; 275:1593. [PubMed: 9054347]
207. Vandecasteele M, Glowinski J, Venance L. *J. Neurosci.* 2005; 25:291. [PubMed: 15647472]



208. Komendantov AO, Canavier CC. *J. Neurophysiol.* 2002; 87:1526. [PubMed: 11877524]
209. Robinson, DL.; Wightman, RM. *Electrochemical Methods for Neuroscience*. Michael, AC.; Borland, LM., editors. Boca Raton: CRC Press; 2007.
210. Venton BJ, Wightman RM. *Synapse.* 2007; 61:37. [PubMed: 17068772]
211. Rebec GV, Christensen JR, Guerra C, Bardo MT. *Brain Res.* 1997; 776:61. [PubMed: 9439796]
212. Garris PA, Christensen JR, Rebec GV, Wightman RM. *J. Neurochem.* 1997; 68:152. [PubMed: 8978721]
213. Robinson DL, Phillips PE, Budygin EA, Trafton BJ, Garris PA, Wightman RM. *Neuroreport.* 2001; 12:2549. [PubMed: 11496146]
214. Robinson DL, Heien ML, Wightman RM. *J. Neurosci.* 2002; 22:10477. [PubMed: 12451147]
215. Wightman RM, Heien ML, Wassum KM, Sombers LA, Aragona BJ, Khan AS, Ariansen JL, Cheer JF, Phillips PE, Carelli RM. *Eur. J. Neurosci.* 2007; 26:2046. [PubMed: 17868375]
216. Pickel VM, Beckley SC, Joh TH, Reis DJ. *Brain Res.* 1981; 225:373. [PubMed: 6118197]
217. Hyland BI, Reynolds JN, Hay J, Perk CG, Miller R. *Neurosci.* 2002; 114:475.
218. Heien ML, Khan AS, Ariansen JL, Cheer JF, Phillips PE, Wassum KM, Wightman RM. *Proc. Natl. Acad. Sci. U. S. A.* 2005; 102:10023. [PubMed: 16006505]
219. Robinson DL, Wightman RM. *J. Neurochem.* 2004; 90:894. [PubMed: 15287895]
220. Stuber GD, Roitman MF, Phillips PE, Carelli RM, Wightman RM. *Neuropsychopharmacol.* 2005; 30:853.
221. Cheer JF, Wassum KM, Heien ML, Phillips PE, Wightman RM. *J. Neurosci.* 2004; 24:4393. [PubMed: 15128853]
222. Cheer JF, Kendall DA, Mason R, Marsden CA. *Neuropharmacol.* 2003; 44:633.
223. French ED, Dillon K, Wu X. *Neuroreport.* 1997; 8:649. [PubMed: 9106740]
224. Cheer JF, Wassum KM, Sombers LA, Heien ML, Ariansen JL, Aragona BJ, Phillips PE, Wightman RM. *J. Neurosci.* 2007; 27:791. [PubMed: 17251418]
225. Pidoplichko VI, DeBiasi M, Williams JT, Dani JA. *Nature.* 1997; 390:401. [PubMed: 9389479]
226. Turner TJ. *J. Neurosci.* 2004; 24:11328. [PubMed: 15601939]
227. Gessa GL, Muntoni F, Collu M, Vargiu L, Mereu G. *Brain Res.* 1985; 348:201. [PubMed: 2998561]
228. Mereu G, Fadda F, Gessa GL. *Brain Res.* 1984; 292:63. [PubMed: 6697212]
229. Shen RY. *J. Pharmacol. Exp. Ther.* 2003; 307:566. [PubMed: 12966156]
230. Pearce, JM. *Animal Learning and Cognition*. 2nd ed.. Erlbaum (UK): Taylor & Francis Ltd.; 1997.
231. Rescorla, RA.; Wagner, AR. *Classical Conditioning II: Current Research and Theory*. Black, AH.; Prokasy, WF., editors. New York: Appleton Century Crofts; 1972.
232. Schultz W, Dickinson A. *Annu. Rev. Neurosci.* 2000; 23:473. [PubMed: 10845072]
233. Mirenovic J, Schultz W. *J. Neurophysiol.* 1994; 72:1024. [PubMed: 7983508]
234. Tobler PN, Dickinson A, Schultz W. *J. Neurosci.* 2003; 23:10402. [PubMed: 14614099]
235. Zhang H, Sulzer D. *J. Neurosci.* 2003; 23:10585. [PubMed: 14627643]
236. Avshalumov MV, Chen BT, Koos T, Tepper JM, Rice ME. *J. Neurosci.* 2005; 25:4222. [PubMed: 15858048]
237. Garris PA, Christensen JRC, Rebec GV, Wightman RM. *J. Neurochem.* 1997; 68:152. [PubMed: 8978721]
238. Phillips PE, Stuber GD, Heien ML, Wightman RM, Carelli RM. *Nature.* 2003; 422:614. [PubMed: 12687000]
239. Stuber GD, Wightman RM, Carelli RM. *Neuron.* 2005; 46:661. [PubMed: 15944133]
240. Day JJ, Roitman MF, Wightman RM, Carelli RM. *Nat. Neurosci.* 2007
241. Ikemoto S, Panksepp J. *Brain Res. Brain Res. Rev.* 1999; 31:6. [PubMed: 10611493]
242. Valenstein ES. *Brain Behav. Evol.* 1969; 2:295.
243. Robinson DL, Heien ML, Wightman RM. *J. Neurosci.* 2002; 22:10477. [PubMed: 12451147]

244. Roitman MF, Stuber GD, Phillips PE, Wightman RM, Carelli RM. *J. Neurosci.* 2004; 24:1265. [PubMed: 14960596]
245. Mahon S, Vautrelle N, Pezard L, Slaght SJ, Deniau JM, Chouvet G, Charpier S. *J. Neurosci.* 2006; 26:12587. [PubMed: 17135420]
246. Armstrong-James M, Millar J, Kruk ZL. *Nature.* 1980; 288:181. [PubMed: 7432519]
247. Williams GV, Millar J. *Neuroscience.* 1990; 39:1. [PubMed: 2089272]
248. Gerhardt GA, Hoffman AF. *J. Neurosci. Methods.* 2001; 109:13. [PubMed: 11489295]
249. Hicks TP. *Prog. Neurobiol.* 1984; 22:185. [PubMed: 6089267]
250. Armstrong-James M, Fox K, Kruk ZL, Millar J. *J. Neurosci. Methods.* 1981; 4:385. [PubMed: 7321578]
251. Bloom FE. *Life Sci.* 1974; 14:1819. [PubMed: 4368008]
252. Neve K, Neve R. *The Dopamine Receptors.* 1997
253. Cheer JF, Aragona BJ, Heien ML, Seipel AT, Carelli RM, Wightman RM. *Neuron.* 2007; 54:237. [PubMed: 17442245]
254. Cheer JF, Heien ML, Garris PA, Carelli RM, Wightman RM. *Proc. Natl. Acad. Sci. U.S.A.* 2005; 102:19150. [PubMed: 16380429]
255. Warenaia MW, McKenzie GM. *Gen. Pharmacol.* 1984; 15:517. [PubMed: 6526262]
256. Greengard P. *Science.* 2001; 294:1024. [PubMed: 11691979]
257. Sealon SC, Olanow CW. *Trends Neurosci.* 2000; 23:S34. [PubMed: 11052218]
258. Nicola SM, Surmeier J, Malenka RC. *Annu. Rev. Neurosci.* 2000; 23:185. [PubMed: 10845063]
259. Svenningsson P, Nishi A, Fisone G, Girault JA, Nairn AC, Greengard P. *Annu. Rev. Pharmacol. Toxicol.* 2004; 44:269. [PubMed: 14744247]
260. Lindskog M, Kim M, Wikstrom MA, Blackwell KT, Kotaleski JH. *PLoS Comput. Biol.* 2006; 2:e119. [PubMed: 16965177]
261. Fienberg AA, Hiroi N, Mermelstein PG, Song W, Snyder GL, Nishi A, Cheramy A, O'Callaghan JP, Miller DB, Cole DG, Corbett R, Haile CN, Cooper DC, Onn SP, Grace AA, Ouimet CC, White FJ, Hyman SE, Surmeier DJ, Girault J, Nestler EJ, Greengard P. *Science.* 1998; 281:838. [PubMed: 9694658]
262. Di Chiara G, Bassareo V, Fenu S, De Luca MA, Spina L, Cadoni C, Acquas E, Carboni E, Valentini V, Lecca D. *Neuropharmacol.* 2004; 47 Suppl 1:227.
263. Sesack SR, Carr DB, Omelchenko N, Pinto A. *Ann. N. Y. Acad. Sci.* 2003; 1003:36. [PubMed: 14684434]
264. Garris PA, Ciolkowski EL, Pastore P, Wightman RM. *J. Neurosci.* 1994; 14:6084. [PubMed: 7931564]
265. Gonon F. *J. Neurosci.* 1997; 17:5972. [PubMed: 9221793]
266. Cardozo DL, Bean BP. *J. Neurophysiol.* 1995; 74:1137. [PubMed: 7500139]
267. O'Hara CM, Uhland-Smith A, O'Malley KL, Todd RD. *J. Pharmacol. Exp. Ther.* 1996; 277:186. [PubMed: 8613917]
268. Onali P, Olanow MC. *Neurosci. Lett.* 1989; 102:91. [PubMed: 2571111]
269. Lindgren N, Xu ZQ, Herrera-Marschitz M, Haycock J, Hokfelt T, Fisone G. *Eur. J. Neurosci.* 2001; 13:773. [PubMed: 11207812]
270. Benoit-Marand M, Borrelli E, Gonon F. *J. Neurosci.* 2001; 21:9134. [PubMed: 11717346]
271. Wu Y, Pearl SM, Zigmond MJ, Michael AC. *Neurosci.* 2000; 96:65.
272. Avshalumov MV, Chen BT, Marshall SP, Pena DM, Rice ME. *J. Neurosci.* 2003; 23:2744. [PubMed: 12684460]
273. Kulagina NV, Zigmond MJ, Michael AC. *Neurosci.* 2001; 102:121.
274. Floresco SB, Blaha CD, Yang CR, Phillips AG. *J. Neurosci.* 2001; 21:6370. [PubMed: 11487660]
275. Howland JG, Taepavarapruk P, Phillips AG. *J. Neurosci.* 2002; 22:1137. [PubMed: 11826142]
276. Zhang H, Sulzer D. *Nature Neurosci.* 2004; 7:581. [PubMed: 15146187]
277. Rice ME, Cragg SJ. *Nature Neurosci.* 2004; 7:583. [PubMed: 15146188]
278. Grace AA, Floresco SB, Goto Y, Lodge DJ. *Trends Neurosci.* 2007

279. West AR, Floresco SB, Charara A, Rosenkranz JA, Grace AA. *Ann. N. Y. Acad. Sci.* 2003; 1003:53. [PubMed: 14684435]
280. Kiyatkin EA, Rebec GV. *J. Neurophysiol.* 1996; 75:142. [PubMed: 8822548]
281. Wickens JR, Wilson CJ. *J. Neurophysiol.* 1998; 79:2358. [PubMed: 9582211]
282. Goto Y, O'Donnell P. *J. Neurosci.* 2001; 21:4498. [PubMed: 11404437]
283. West AR, Grace AA. *J. Neurosci.* 2002; 22:294. [PubMed: 11756513]
284. Levine MS, Altemus KL, Cepeda C, Cromwell HC, Crawford C, Ariano MA, Drago J, Sibley DR, Westphal H. *J. Neurosci.* 1996; 16:5870. [PubMed: 8795639]
285. Cepeda C, Buchwald NA, Levine MS. *Proc. Natl. Acad. Sci. U.S.A.* 1993; 90:9576. [PubMed: 7692449]
286. Surmeier DJ, Bargas J, Hemmings HC Jr, Nairn AC, Greengard P. *Neuron.* 1995; 14:385. [PubMed: 7531987]
287. Hernandez-Lopez S, Tkatch T, Perez-Garci E, Galarraga E, Bargas J, Hamm H, Surmeier DJ. *J. Neurosci.* 2000; 20:8987. [PubMed: 11124974]
288. Kiyatkin EA, Rebec GV. *Brain Res.* 1997; 771:14. [PubMed: 9383003]
289. Gonon F, Sundstrom L. *Neurosci.* 1996; 75:13.
290. Hu XT, White FJ. *Neurosci. Lett.* 1997; 224:61. [PubMed: 9132692]
291. Bamford NS, Zhang H, Schmitz Y, Wu NP, Cepeda C, Levine MS, Schmauss C, Zakharenko SS, Zablow L, Sulzer D. *Neuron.* 2004; 42:653. [PubMed: 15157425]
292. Trudeau LE. *J. Psychiat. Neurosci.* 2004; 29:296.
293. Kawano M, Kawasaki A, Sakata-Haga H, Fukui Y, Kawano H, Nogami H, Hisano S. *J. Compar. Neurol.* 2006; 498:581.
294. Lapish CC, Seamans JK, Judson Chandler L. *Alcohol Clin. Exp. Res.* 2006; 30:1451. [PubMed: 16930207]
295. Freneau RT, Burman J, Qureshi T, Tran CH, Proctor J, Johnson J, Zhang H, Sulzer D, Copenhagen DR, Storm-Mathisen J, Reimer RJ, Chaudhry FA, Edwards RH. *Proc. Natl. Aca. Sci. U.S.A.* 2002; 99:14488.
296. Herzog E, Gilchrist J, Gras C, Muzerelle A, Ravassard P, Giros B, Gaspar P, EL Mestikawy S. *Neurosci.* 2004; 123:983.
297. Sulzer D, Joyce MP, Lin L, Geldwert D, Haber SN, Hattori T, Rayport S. *J. Neurosci.* 1998; 18:4588. [PubMed: 9614234]
298. Chuhma N, Zhang H, Masson J, Zhuang X, Sulzer D, Hen R, Rayport S. *J. Neurosci.* 2004; 24:972. [PubMed: 14749442]
299. Bert L, Parrot S, Robert F, Desvignes C, Denoroy L, Suaud-Chagny MF, Renaud B. *Neuropharmacol.* 2002; 43:825.
300. Bowser MT, Kennedy RT. *Electrophoresis.* 2001; 22:3668. [PubMed: 11699904]
301. Wei H, Nolkranz K, Parkin MC, Chisolm CN, O'Callaghan JP, Kennedy RT. *Anal. Chem.* 2006; 78:4342. [PubMed: 16808441]
302. O'Brien KB, Esguerra M, Miller RF, Bowser MT. *Anal. Chem.* 2004; 76:5069. [PubMed: 15373444]
303. Ciriacks CM, Bowser MT. *Anal. Chem.* 2004; 76:6582. [PubMed: 15538780]
304. Shou M, Ferrario CR, Schultz KN, Robinson TE, Kennedy RT. *Anal. Chem.* 2006; 78:6717. [PubMed: 17007489]
305. Venton BJ, Robinson TE, Kennedy RT. *J. Neurochem.* 2006; 96:236. [PubMed: 16300631]
306. Sandlin ZD, Shou M, Shackman JG, Kennedy RT. *Anal. Chem.* 2005; 77:7702. [PubMed: 16316179]
307. Cellar NA, Burns ST, Meiners JC, Chen H, Kennedy RT. *Anal. Chem.* 2005; 77:7067. [PubMed: 16255611]
308. Kottegoda S, Shaik I, Shippy SA. *J. Neurosci. Methods.* 2002; 121:93. [PubMed: 12393165]
309. Ramesh P, Sampath S. *Electroanalysis.* 2004; 16:866.
310. Ciszewski A, Milczarek G, Kubaszewski E, Lozynski M. *Electroanalysis.* 1998; 10:628.
311. Phillips PEM, Wightman RM. *Trends Anal. Chem.* 2003; 22:509.

312. Jones SR, Garris PA, Wightman RM. *J. Pharmacol. Exp. Ther.* 1995; 274:396. [PubMed: 7616424]
313. Schultz W. *J. Neurophysiol.* 1998; 80:1. [PubMed: 9658025]

## Biographies





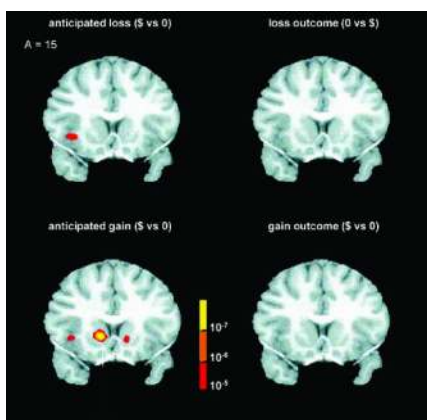


**Figure 1.** Data taken from Knutson et al., 2003<sup>28</sup> showing blood oxygen-level-dependent signals recorded from a human subject playing a neuroeconomic game. Note that the region highlighted in the panel labeled anticipated gain is the nucleus accumbens, a region that uses dopamine as a neurotransmitter. Reprinted with permission; copyright 2003, Elsevier.



**Figure 2.**

Diagram of fast scan cyclic voltammetry of dopamine. A range of potentials such as the triangle waveform (top left) is applied to the carbon-fiber microelectrode (center). During the anodic scan dopamine oxidizes, and on the cathodic scan dopamine-*o*-quinone reduces. The resulting current is measured as a cyclic voltammogram; the voltammogram shown here (right) is background-subtracted to reveal the current due to dopamine oxidation and reduction. Reprinted with permission from<sup>311</sup>. Copyright 2003, Elsevier.

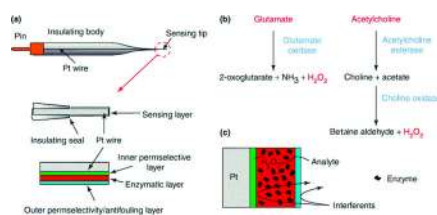


**Figure 3.**

Principles underlying enzymatic, amperometric microelectrode biosensors. (a) A microelectrode biosensor will generally have a rigid insulating body with a pin at one end for connection to the potentiostat and the fine sensing tip at the other. A Pt wire connected to the pin emerges from the tip of the body to give a defined sensing area. The sensing area is then coated with a special layer, which at the very minimum comprises the enzymatic layer. In some designs, there can be inner and outer selectively permeable layers to exclude electroactive interferences and reduce fouling of the sensor. (b) Examples of two enzymatic cascades used to measure signaling by glutamate and acetylcholine in the brain. Note that the analyte is converted into an electrochemically active product – in this case H<sub>2</sub>O<sub>2</sub> – that can be detected by the microelectrode. (c) The analyte of interest diffuses into the enzymatic layer and is catalyzed by the enzymes to peroxide; this then diffuses to the electrode surface through any inner selectively permeable layers. However, interferences can be rejected either by an outer layer, such as cellulose acetate, or by an inner layer, such as Nafion. Adapted from reference<sup>176</sup> with permission. Copyright 2005, Elsevier.



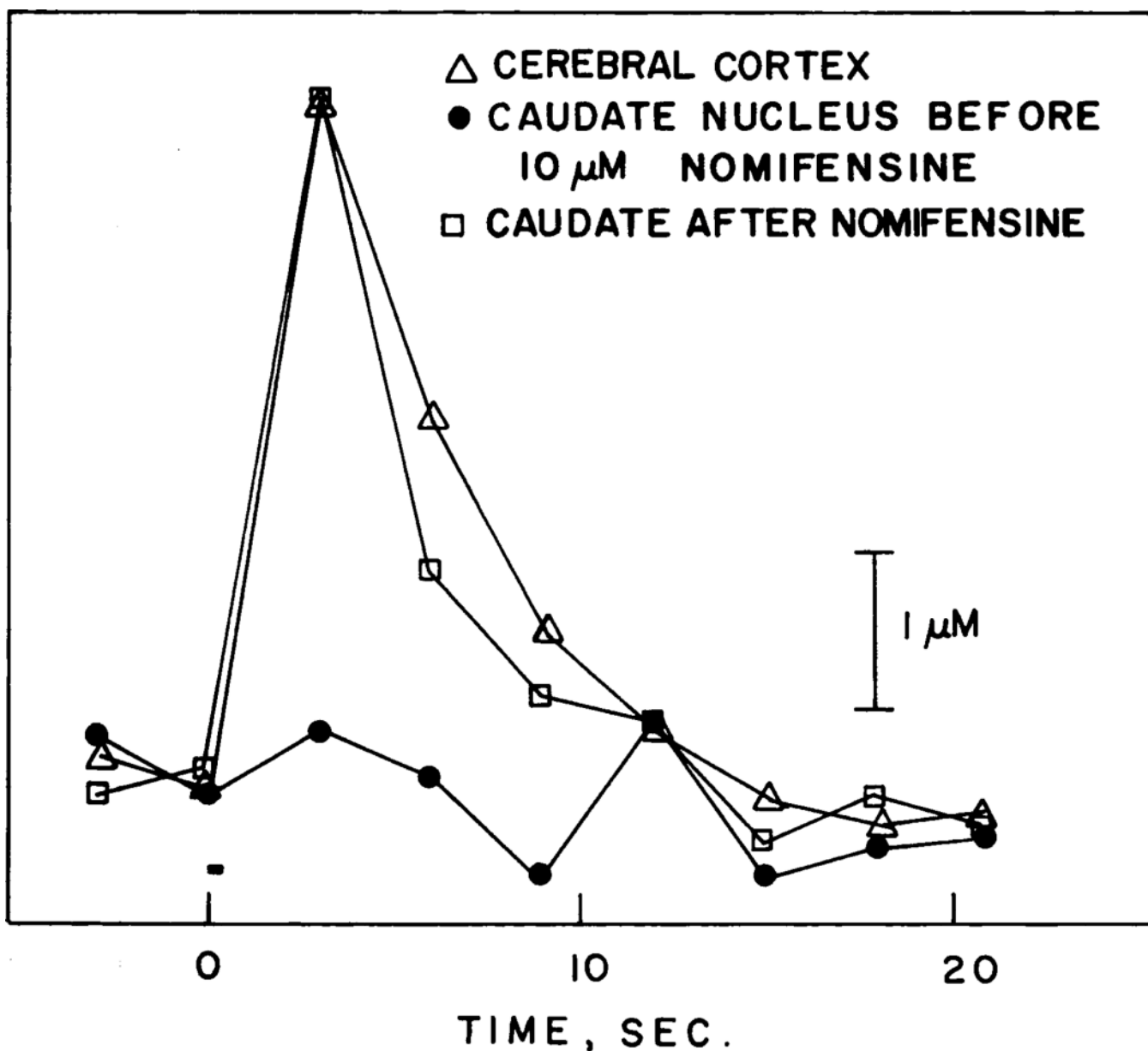


**Figure 4.** Pressure ejection of dopamine into the slice as detected with an adjacent voltammetric electrode. The tip of the pipette was secured at a 70  $\mu\text{m}$  distance from the working electrode. First, dopamine was ejected from a pipette into the cortex. The entire assembly was then raised and lowered into the caudate nucleus and the ejection repeated. Dopamine was only observed in the caudate nucleus after the slice had been perfused with 10  $\mu\text{M}$  nomifensine, a dopamine uptake blocker. Reprinted with permission from<sup>181</sup>. Copyright 1989 Elsevier.

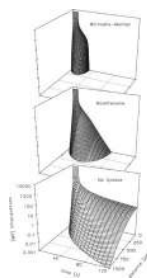


**Figure 5.**

Three-dimensional plots of concentration as function of distance and time for three different uptake conditions. All calculations were based on a numerical solution of Fick's second law coupled to the Michaelis-Menten equation. Iontophoresis lasted for the first 10 s. The upper graph was computed with  $V_{\max} = 0.2, \text{ uM s}^{-1}$ ,  $K_m = 0.15 \text{ }\mu\text{M}$ , i.e., standard Michaelis-Menten parameters. The middle graph was computed with  $V_{\max} = 0.2, \text{ uM s}^{-1}$ ,  $K_m = 6.0 \text{ }\mu\text{M}$ , i.e., as if uptake was inhibited by an agent like nomifensine. The bottom graph was computed with  $V_{\max} = 0$ , i.e., with no uptake. Reprinted with permission from<sup>184</sup>. Copyright 1995 Biophysical Society

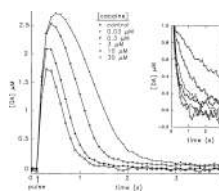


**Figure 6.** Effects of increasing concentrations of cocaine on one-pulse stimulated dopamine efflux in a single brain slice containing the caudate nucleus. Data was collected in a single electrode placement area of the slice by using a cumulative dosing regimen. Increasing doses were added at 30-min intervals at the concentrations indicated. Arrow, the time when the stimulus pulse was applied. Symbols are data points, collected every 100 ms, and lines connect the symbols for clarity. INSET: disappearance of dopamine after stimulation. Data was time-shifted so that the initial dopamine concentration was 1  $\mu\text{M}$  for each plot. Reprinted with permission from<sup>312</sup>. Copyright 1995 American Society for Pharmacology and Experimental Therapeutics.

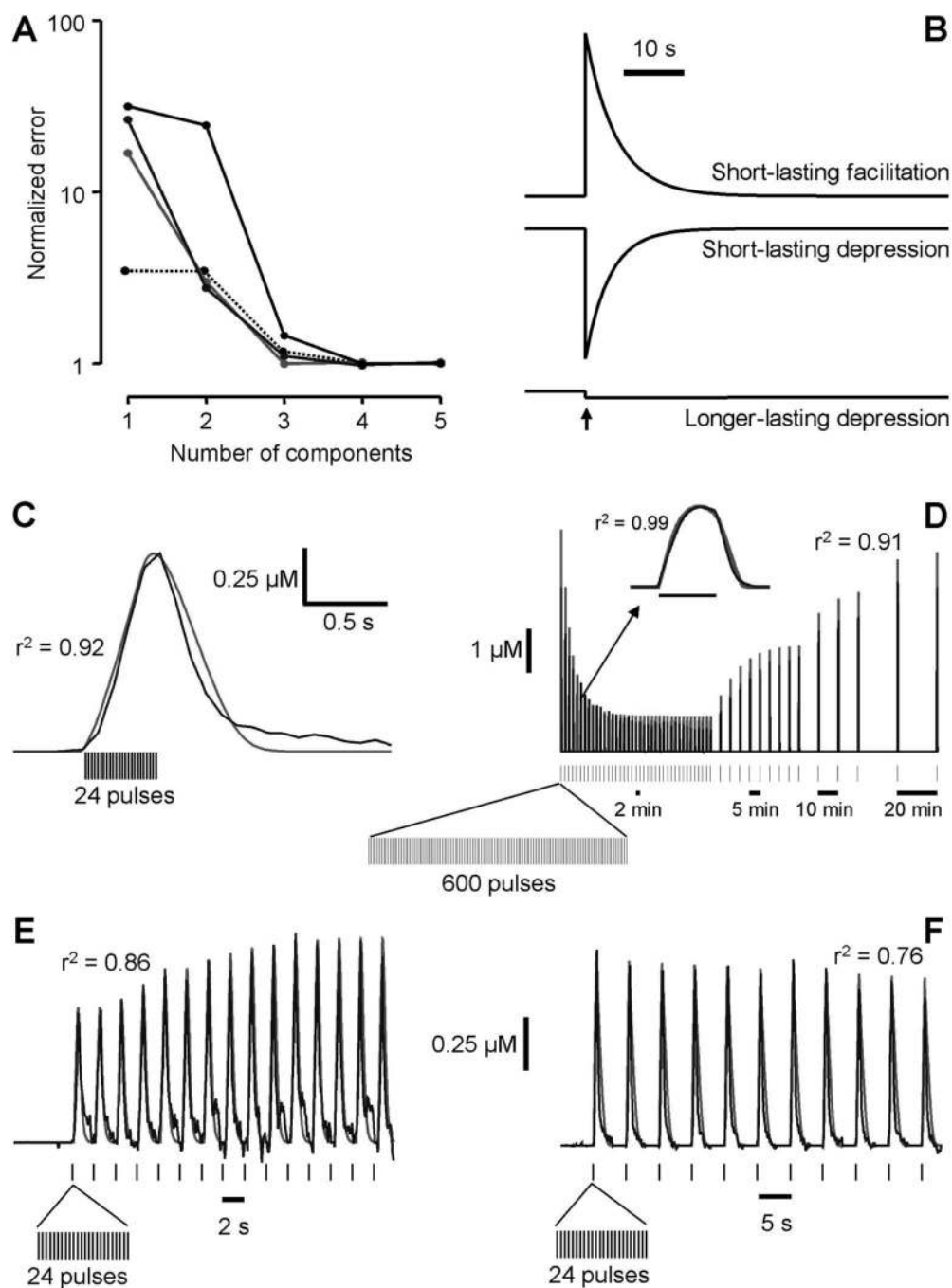


**Figure 7.** Dynamic model reveals multiple adaptive mechanisms for ongoing dopamine release. **A**, Semi-log plot of the normalized error for fitting the model to experimental data versus the number of independent dynamic components  $I_j$ . Representative fits are shown from four representative animals. The error decreases up to three components and does not improve appreciably beyond that. **B**, The three dynamic components consistently captured by the model: short-lasting facilitation (top), short-lasting depression (middle), and longer-lasting depression (bottom). These time-dependent mathematical components are induced by each action potential (arrow) and multiplicatively modify the amplitude of dopamine release for future action potentials. **C**, Fit of dynamic model to dopamine released during a single

repetitive electrical stimulation (24 pulses, 60 Hz, 120  $\mu$ A) applied to dopamine neurons of an ambulant rat. In all panels, the model is grey, data are black, and  $r^2$  is the correlation coefficient. D, Fit of model to dopamine fluctuations evoked in an anesthetized animal by more intense stimulus trains. Each repetitive stimulus (vertical bar) consisted of 600 pulses (60 Hz, 120  $\mu$ A). The repetitive stimulus trains were delivered at 2, 5, 10, or 20 min intervals. Depression is present that is still evident on the next stimulus with 2 min interstimulus intervals. At longer intervals there is greater recovery of release. Inset, Response for a single 600 pulse train (60 Hz, 120  $\mu$ A). E, Fit of model to dopamine fluctuations evoked by stimuli as in C repeated at 2 sec intervals. Facilitation is apparent. F, Stimuli as in C repeated at 5 sec intervals. A gradual depression is apparent. Reprinted with permission from<sup>201</sup>. Copyright 2004 Society for Neuroscience.

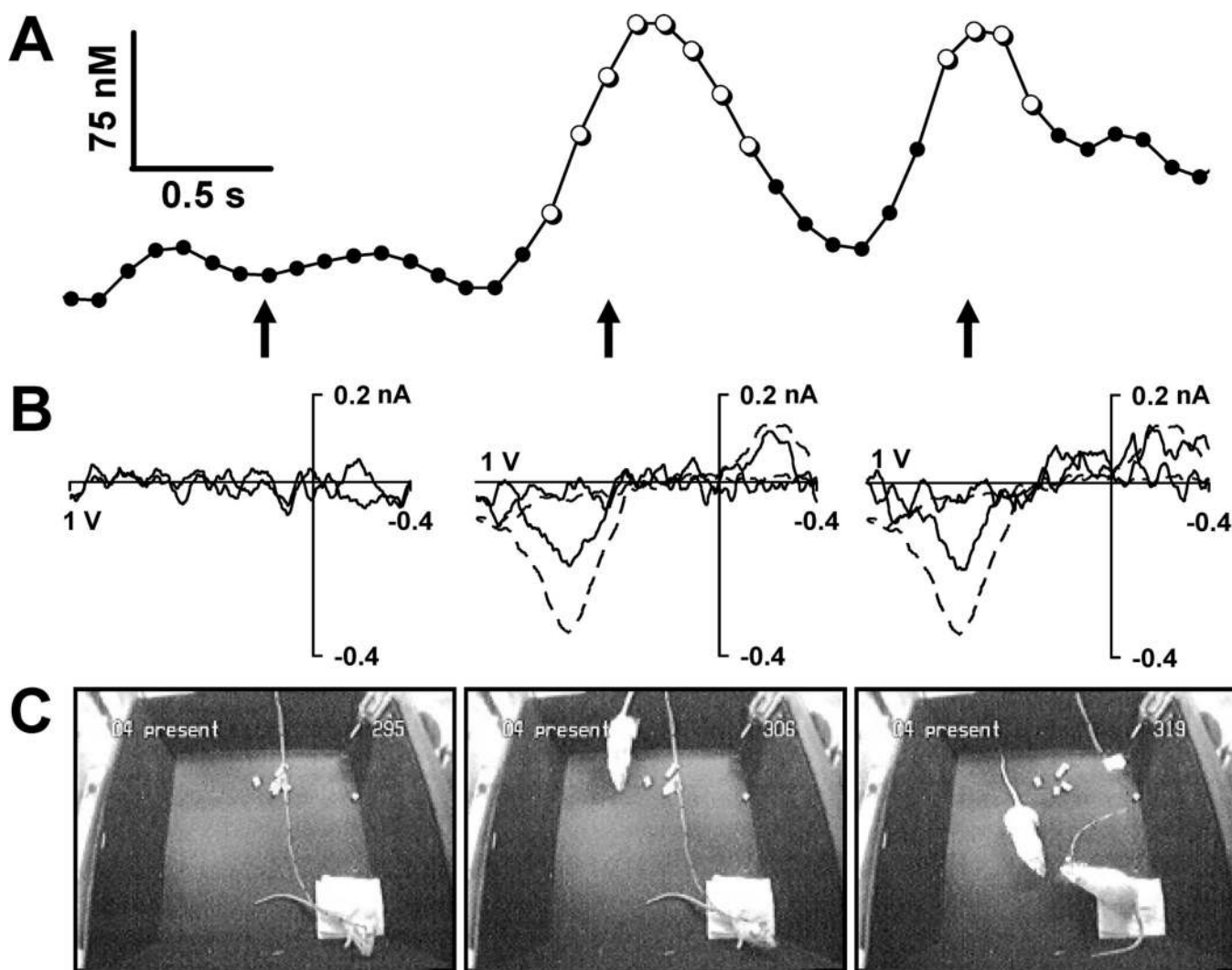


**Figure 8.**

Two dopamine concentration transients in the olfactory tubercle of a male rat associated with the introduction of a receptive female to the test chamber and subsequent contact. A, A 4-sec trace of the electrochemical signal at the oxidation potential of dopamine (0.6 V versus Ag/AgCl reference) converted to dopamine concentration using the *in vitro* calibration of the electrode after the experiment. The electrochemical scans confirmed to be dopamine by the cyclic voltammograms are indicated by open circles. B, Cyclic voltammograms corresponding to the electrochemical signal at the times indicated by the arrows. The cyclic voltammograms verify that the changes in electrochemical signal during the two transients are attributable to the oxidation of dopamine (middle and right), whereas no changes in dopamine are apparent beforehand (left). The oxidative and reductive peaks of the dopamine transients are compared with those of dopamine obtained during the electrical stimulation of the dopamine fibers (dotted line, scaled to size). C, The video record of the experiment corresponding to the electrochemical signal at the times indicated by the arrows. The first dopamine transient coincided with the entrance of the female to the test chamber and was followed by immediate orientation of the male toward the female. The second transient was concurrent with the initial whisker contact between the rats and was followed by investigative sniffing of the female by the male. Reprinted with permission from<sup>214</sup>. Copyright 2002 Society for Neuroscience.

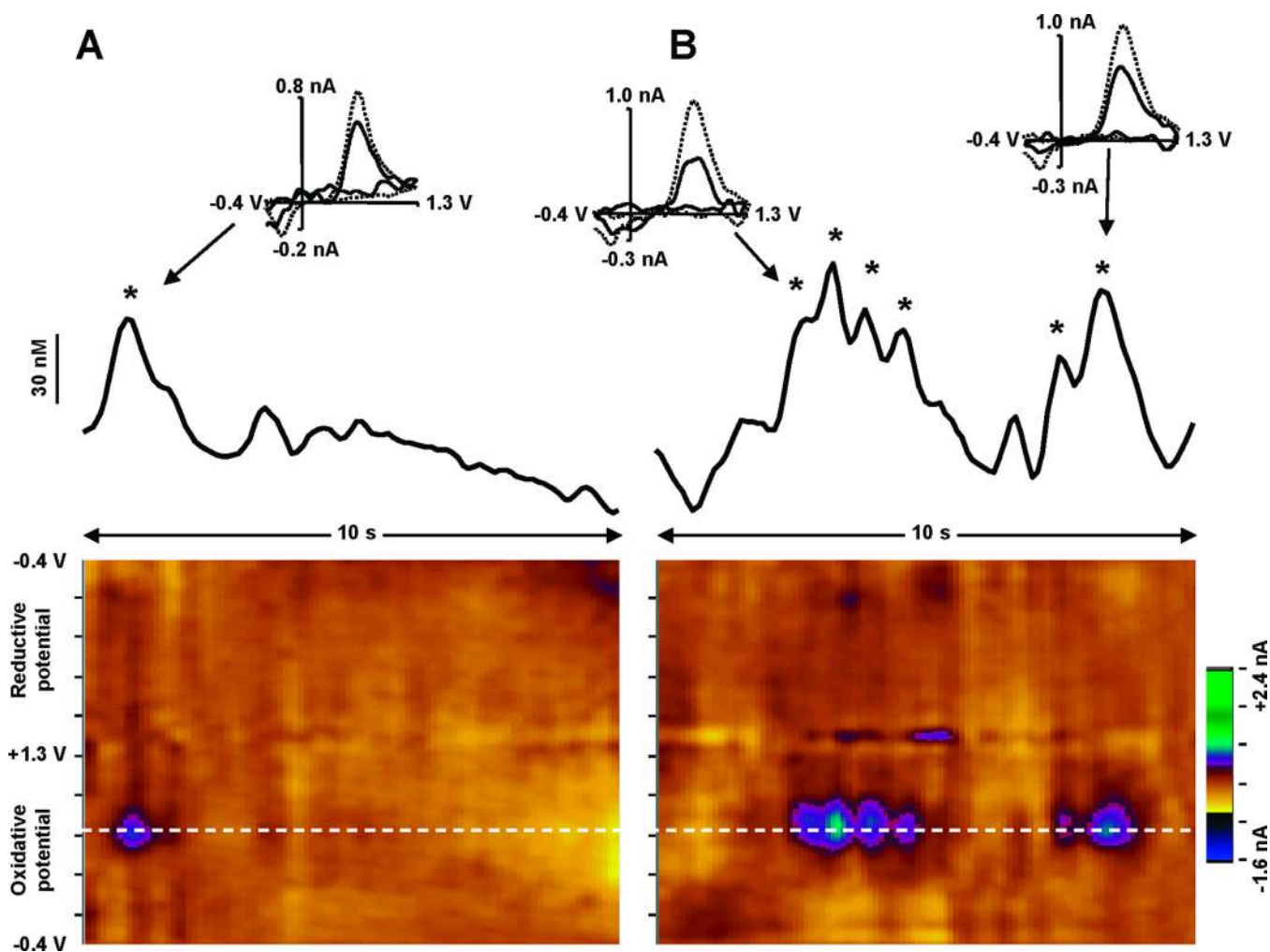


**Figure 9.** Representative recordings of dopamine transients in a site in the nucleus accumbens supporting few dopamine transients (A) and in one supporting frequent transients (B), recorded in separate rats. The color plot<sup>132</sup> (bottom) illustrates changes in current (color) by applied potential (y-axis) over a 10-s window (x-axis). Changes in current at the oxidation potential of dopamine, indicated on the color plot by the white dotted line, are shown in the trace above the color plot. Increases in current confirmed to be due to dopamine oxidation (dopamine transients) are designated by the asterisks. Cyclic voltammograms of selected dopamine transients (solid lines) are shown above the traces, along with electrically stimulated dopamine signals from the same site (scaled to the dopamine transient, dotted lines).

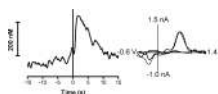


**Figure 10.**

Dopamine transients during cocaine self-administration. Left panel: dopamine increases before the lever press (time 0, solid line) and immediately after. Right panel: the cyclic voltammogram indicates the substance detected was dopamine. The solid line is the cyclic voltammogram taken at the peak of the dopamine response, and the dashed line is the cyclic voltammogram taken during electrical stimulation of the ventral tegmental area (24 pulses, 125  $\mu$ A, at 60 Hz) normalized to the peak amplitude for the response at the lever press.



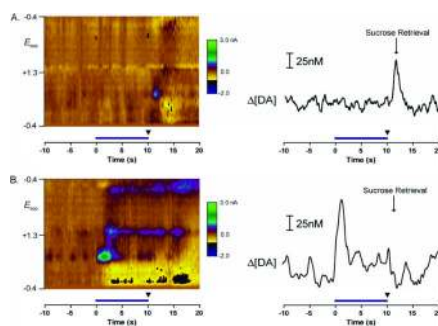


**Figure 11.** Voltammetric responses during a behavioral task measured in the rat nucleus accumbens. At time 0 in both panels a lever was extended and it was retracted after 10s (blue bar). Subsequently a sucrose pellet was dispensed. A. Results from a single animal on the first day. Note the dopamine transient occurs with sucrose retrieval. B. After 10 days of training the dopamine transient occurs with the lever extension, the cue that predicts the later delivery of sucrose. Adapted from reference<sup>240</sup>.

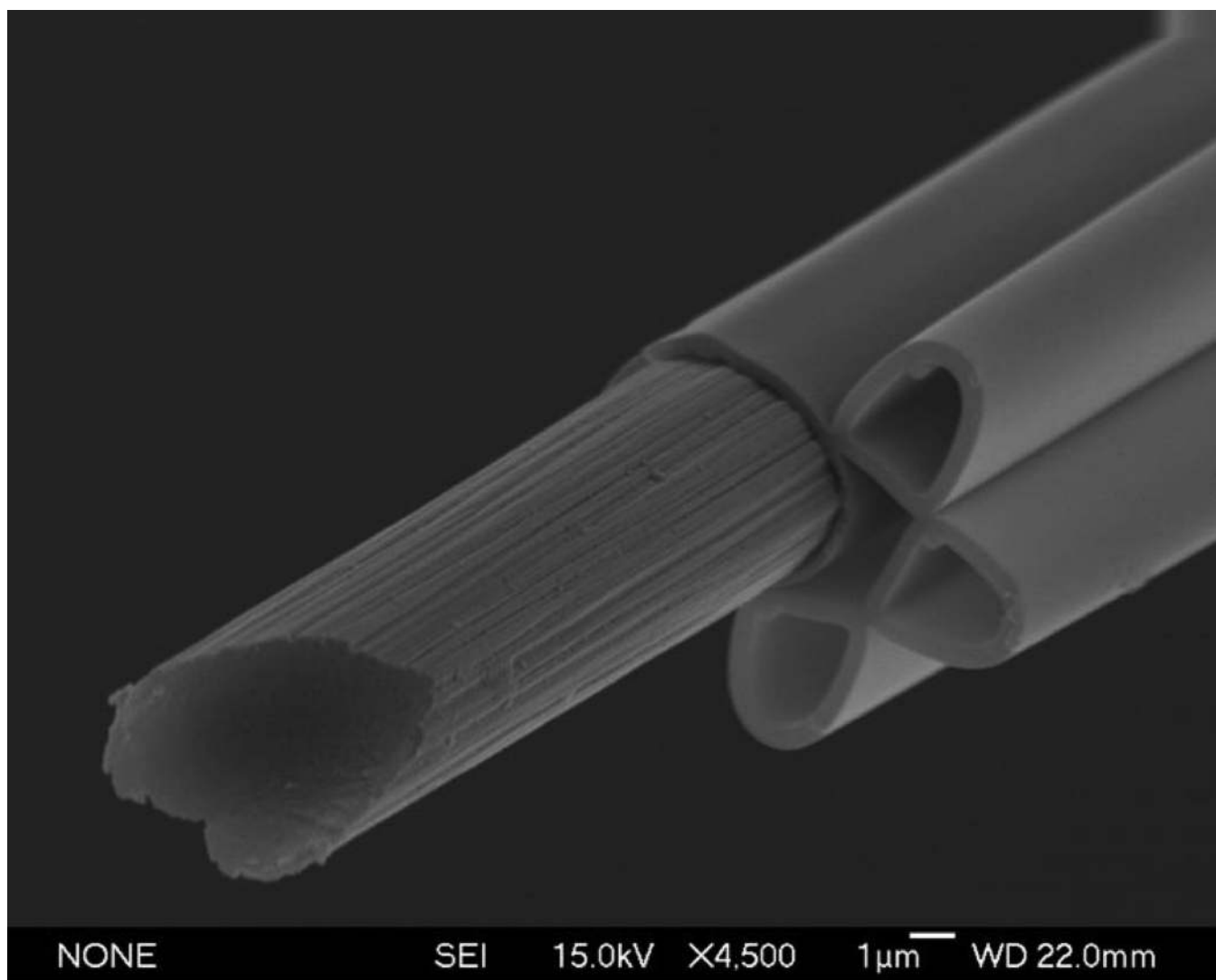


**Figure 12.** Carbon-fiber electrode fabricated with three barrels for iontophoresis. Note the filament within the capillaries—this acts as a wick to aid in filling the barrels.

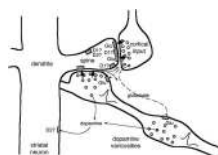


**Figure 13.**

Influences of dopamine release on typical medium spiny neurons in the dorsal and ventral striatum. Dopamine released by impulses from synaptic varicosities activates a few synaptic receptors (probably of D2 type in the low-affinity state) and diffuses rapidly out of the synapse to reach low affinity D1 type receptors that are located nearby, within corticostriatal synapses, or at a limited distance. Phasically increased dopamine activates nearby high-affinity D2 type receptors to saturation. D2 receptors remain partly activated by the ambient dopamine concentrations after the phasically increased release. Extrasynaptically released dopamine may get diluted by diffusion and activate high-affinity D2 receptors. It should be noted that, in variance with this schematic diagram, most D1 and D2 receptors are located on different neurons. Glutamate released from corticostriatal terminals reaches postsynaptic receptors located on the same dendritic spines as dopamine varicosities. Glutamate also reaches presynaptic dopamine varicosities where it controls dopamine release. Dopamine influences on spiny neurons in frontal cortex are comparable in many respects. Reprinted with permission from reference<sup>313</sup>. Copyright 1998 American Physiological Society.

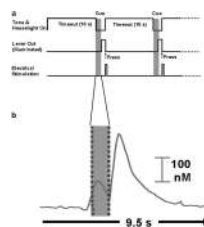


**Figure 14.** Dopamine responses during intracranial self-stimulation. A. Timing diagram for lever extension, audiovisual cue, and electrical stimulation. B. Dopamine responses measured by cyclic voltammetry and extracted with principal component regression. Reprinted with permission from reference<sup>253</sup>. Copyright 2007 Elsevier.

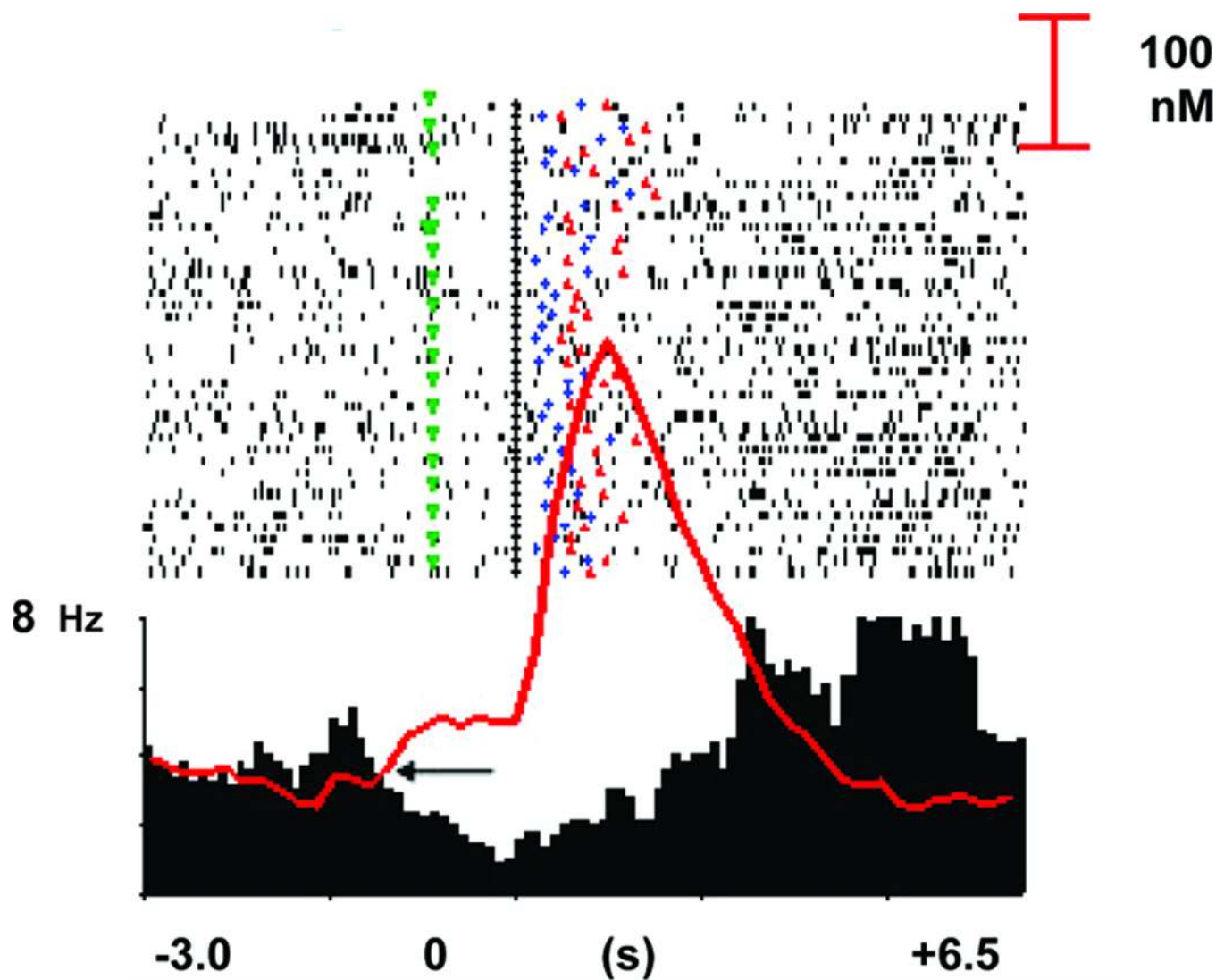


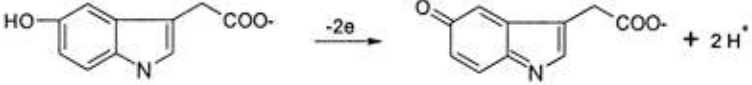
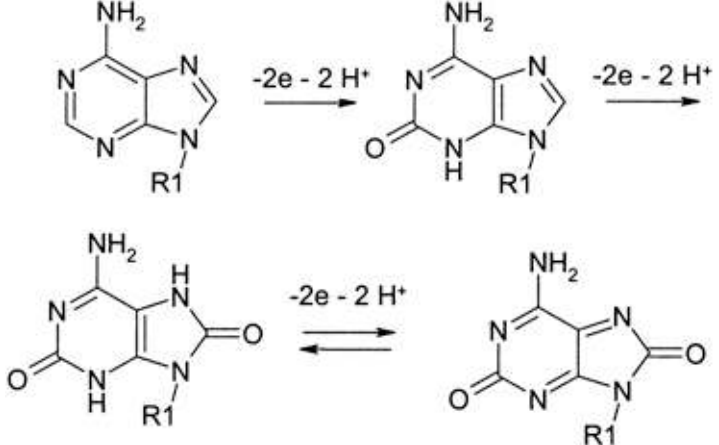
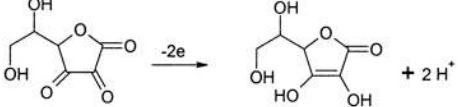
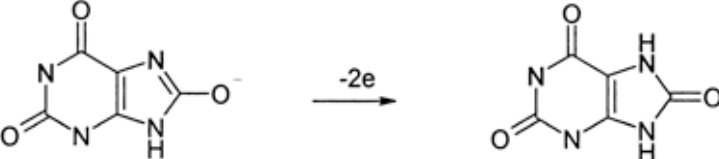
**Figure 15.**

Simultaneous measurement of firing patterns of neurons in the nucleus accumbens with subsecond dopamine changes measured at the same electrode during intracranial self stimulation. The peri-event histogram was obtained by summing single unit events recorded from a single neuron over individual trials. The overlaid trace (red) shows the time course of single-session extracellular dopamine concentration changes simultaneously measured at the same loci where neurons were recorded. Cue onset, green symbols; lever extension, black symbols; lever press, blue crosses; lever press; red dots are the stimulus delivery. The arrow indicates where unit activity and dopamine simultaneously change. Adapted from<sup>253</sup> with permission. Copyright 2007 Elsevier.

Table 1

Redox reactions for electrochemically detectable molecules present in the brain

Molecule	Redox-Reaction	Approximate peak potential <i>in vivo</i> <sup>32</sup> at physiological pH (vs Ag/AgCl)
Tyrosine derivatives		+0.7 V
L-DOPA		+0.4 V
Dopamine		+0.2 V
Norepinephrine		+0.2 V
Epinephrine		+0.2 V
DOPAC		+0.2 V
Homovanilic Acid		+0.5 V
3-Methoxytyramine		+0.5 V
Tryptophan derivatives		+0.8 V
Serotonin		+0.35 V

Molecule	Redox-Reaction	Approximate peak potential <i>in vivo</i> <sup>32</sup> at physiological pH (vs Ag/AgCl)
5-Hydroxyindolacetic acid		+0.35 V
Other electroactive molecules		
Adenosine <sup>48</sup>		First step +1.2 V
Ascorbic Acid		+0.2 V
Uric acid <sup>309</sup>		+0.3 V